International Journal of Hydrogen Energy 55 (2024) 1143–1160

Contents lists available at ScienceDirect

International Journal of Hydrogen Energy

journal homepage: www.elsevier.com/locate/he

Hydrogen production via steam reforming of different fuels: thermodynamic comparison

Alessandra Di Nardo *, Maria Portarapillo, Danilo Russo, Almerinda Di Benedetto

Department of Chemical, Materials and Production Engineering, University of Naples Federico II, P.le Tecchio 80, 80125, Naples, Italy

ARTICLE INFO

HANDLING EDITOR: Dr. E.A. Veziroglu

Keywords:
Hydrogen
Steam reforming
Thermodynamic analysis
Bio-alcohols
Glycerol
Propane

ABSTRACT

Hydrogen, a sustainable energy source, has potential to address climate change. However, traditional steam reforming processes produce CO_2. Alternative fuels like bio-alcohols, biogas, and LPG are being adopted for steam reforming processes. This study presents a thermodynamic comparative examination of steam reforming processes employing different fuels, including methane, methanol, ethanol, propane, glycerol, and biogas. The analysis focuses on the hydrogen yield, environmental impact, and energy requirements of these processes and a comparison with experimental results. The analyses were conducted using AspenPlus® software, minimizing the Gibbs free energy under specified conditions (T = 25–1000 °C, n = 1–10, P = 1–40 bar). Among the fuels examined, methanol, biogas, and methane exhibited the highest hydrogen yields, reaching maximum values of 96.10 %, 95.86 %, and 95.26 % respectively at 600 °C, 1 bar, and a water-to-fuel ratio of 10. Ethanol, glycerol, and propane achieved yields of 89.66 %, 86.55 %, and 84.03 % respectively at 700 °C and the same pressure and water-to-fuel ratio.

1. Introduction

Hydrogen is emerging as an ideal sustainable energy carrier, offering a more environmentally friendly option for energy consumption. No carbon emissions and little release of other harmful gases result from its use in fuel cells or combustion plants [1,2]. Hydrogen is a promising energy source for long-term sustainable development because of its higher mass energy density compared to other fuels, high energy conversion efficiency, emission-free production via water electrolysis, various storage forms (such as gaseous, liquid, or metal hydrides), simplicity of conversion into other energy forms, and wide availability [3,4]. Despite the benefits highlighted, there are still certain difficulties associated with its manufacture, storage, and distribution [5,6].

Producing hydrogen from naturally occurring substances incurs a substantial energy cost, making it an acknowledged energy carrier [1]. Currently, almost all hydrogen is produced by fossil fuels, which account for about 6 % and 2 % of global natural gas and coal consumption, respectively [7]. Natural gas reforming generates nearly 95 % of H_2, with significant CO_2 emissions, 8 Kg CO_2/Kg H_2, and a minimum energy demand of 62 kJ/mol H_2 [8,9]. Therefore, it has been viewed as a highly essential strategy in recent years to develop hydrogen generation technologies using alternative and renewable energy sources [10].

The escalating costs of fossil fuels, driven by their finite reserves, alongside the rising concentration of CO_2 in the atmosphere resulting from their utilization, have sparked an increasing interest in utilizing biomass for sustainable energy and chemical production [11]. Since they are carbon neutral, biomass-derived alcohols (methanol, ethanol, glycerol) are interesting sources of hydrogen [12]. The product distribution can be affected by the quantity and the arrangement of hydroxyl groups present in the starting alcohol [11,13]. Bio-methanol (CH_3OH) is usually produced via the thermochemical route of biorefinery processes from carbon-based material such as biomass, solid waste, coal, or carbon dioxide. In these processes, the gasification of carbonaceous feedstocks generate biogas, which is subsequently purified and pre-processed before being utilized in the synthesis of methanol [14]. In recent years, bioethanol (C_2H_5OH) has become the most widely used biofuel worldwide, primarily sourced from agricultural raw materials like corn or sugar cane. However, the development of upcoming biorefinery technologies focused on waste-derived it is anticipated that the upcoming generation of biorefinery technologies, focusing on utilizing waste-derived feedstocks, will soon be able to reduce the need for bioethanol from food [10,14]. Glycerol ($C_3H_8O_3$) emerges as a viable option among various renewable feedstocks due to its notable characteristics. It boasts a relatively high hydrogen content, it is nontoxic, and can be safely stored and handled [11]. Approximately 10 % (w/w) of glycerol is

* Corresponding author.
E-mail address: alessandra.dinardo@unina.it (A. Di Nardo).

https://doi.org/10.1016/j.ijhydene.2023.11.215
Received 7 July 2023; Received in revised form 14 November 2023; Accepted 19 November 2023
Available online 25 November 2023

Abbreviation

SRM	Methane Steam Reforming
SR	Steam Reforming
WGS	Water-Gas Shift
DRM	Dry Methane Reforming
POx	Partial Oxidation
ATR	Autothermal reforming
SE-SRM	Sorbent Enhanced Methane Steam Reforming
CL-SRM	Chemical Looping Methane Steam Reforming
SRMe	Methanol Steam Reforming
SRE	Ethanol Steam Reforming
SRG	Glycerol Steam Reforming
LPG	Liquid Petroleum Gas
SRP	Propane Steam Reforming
SRB	Biogas Steam Reforming
rWGS	Reverse Water-Gas Shift
M	Mixer
HE	Heat Exchanger
R	Reactor

Symbols

n	Water-to-fuel ratio
P	Pressure (bar)
T	Temperature (°C)
n_{stoic}	Stoichiometric value of water-to-fuel ratio for overall steam reforming reaction
X_{eq}	Equilibrium conversion of fuel
$F_{fuel,in}$	Molar flow rates of the fuel at reactor inlet (Kmol/h)
$F_{fuel,out}$	Molar flow rates of the fuel at reactor outlet (Kmol/h)
Y_{H_2}	Hydrogen yield
$F_{H_2,out}$	Molar flow rates of hydrogen at reactor outlet (Kmol/h)
S_{H_2}	Hydrogen selectivity
$F_{H_2O,in}$	Molar flow rates of steam at reactor inlet (Kmol/h)
$F_{H_2O,out}$	Molar flow rates of steam at reactor outlet (Kmol/h)
ν_{H_2}	Stoichiometric coefficient of hydrogen in the overall steam reforming reaction
Q_R	Duty at reactor (Kcal/h)
Q_{HE}	Duty at heat exchanger (Kcal/h)
Q	Total duty (Kcal/h)
T_R	Temperature at reactor (°C)
T_{IN}	Temperature at reactor inlet (°C)
$m_{CO_2,flue\ gases}$	Mass flow rates of CO_2 in flue gases (Kg/h)
$m_{CO_2,R}$	Mass flow rates of CO_2 at reactor outlet (Kg/h)
n_{H_2}	Molar flow rate of H_2 (Kmol/h)
m_{CO_2}	Total mass flow rates of CO_2 (Kg/h)
$T_{\Delta G^\circ=0}$	Temperature at which $\Delta G^\circ = 0$ (K)

obtained as a by-product during the conversion of vegetable oil into biodiesel through the transesterification reaction. The market value of pure glycerol currently ranges from $0.27 to $0.41 per pound, while crude glycerol with an 80 % purity fetches around $0.04–0.09 per pound. This price disparity underscores the impact of glycerol oversupply in the market. Therefore, a significant issue in the biodiesel sector is the use of crude glycerol for value-added products. The contaminants in raw glycerol make it very difficult to transform it into a product with value. To avoid market saturation and boost revenues from the manufacture of biodiesel, it is crucial to purify crude glycerol or discover a technique to valorise it [15,16]. Pure glycerol finds applications in various industries, including personal care products, food, oral care, tobacco, and polyurethane manufacturing [17].

As already mentioned, natural gas is the preferred feedstock for producing hydrogen since it is readily available and favourable prices. Compared to feedstocks with higher hydrocarbon content such as liquefied petroleum gas (LPG) or naphtha, sweetening of the feedstock as well as the deactivation of the catalyst are less relevant and easier to address. However, depending on local availability and pricing, hydrocarbons with higher carbon atoms content than natural gas are adopted in many regions because they are cleaner and contain a higher percentage of hydrogen by weight [18]. LPG primarily consists of propane (C_3H_8) and butane (C_4H_{10}), although their volume percentages can vary based on different standards and climates in different countries. For instance, although LPG produced in Korea often contains 65 %–90 % butane, LPG manufactured in Canada typically has 92.5 %–100 % propane [19]. Among the various sources of hydrogen, such as hydrocarbons and alcohols, propane is of special interest. This is primarily due to its unique ability to undergo liquefaction at ordinary temperatures and approximately 9 bar pressure. Consequently, propane offers advantages in terms of effortless storage, transportation, and convenient access, thanks to the existing infrastructure for liquefied petroleum gas [20].

The scientific community has displayed significant interest in advancing biogas as an alternative solution to replace fossil fuels in the transition towards a hydrogen-based economy. Biogas, acknowledged as an eco-friendly and renewable gaseous fuel, holds great promise for direct conversion into syngas through the reforming process [21]. This renewable fuel is produced via the anaerobic digestion of organic matter like liquid manure, sewage sludge, and the organic component present in household and industrial waste. The biogas composition is dependent on the waste source utilized. Typical composition ranges are: CH_4 (60–70 vol%) and CO_2 (30–40 vol%), with small fractions of other compounds such as N_2 (0–2 vol%), CO (<0.5 %), H_2S (0.005–2 %), O_2 (0–5 %), NH_3 (<1 %) [21,22].

As described earlier, steam reforming for hydrogen production requires complex reaction mechanisms for each fuel. Consequently, it results in the production of various by-products, which have implications for the purity of the final hydrogen output and the overall costs involved. Furthermore, the yield of hydrogen is influenced by multiple process variables, including pressure, temperature, and the water-to-fuel ratio. Furthermore, steam reforming is an energy-intensive reaction that necessitates a substantial amount of heat, often generated through the combustion of auxiliary streams. This supplementary energy consumption contributes to the overall CO_2 emissions associated with the process. This aspect related to the energy demand is fundamental to the development of hydrogen production processes from alternative feedstocks and is not usually considered in the literature.

Therefore, the present work aims to collect and compare thermodynamic data of the main alternative fuels for hydrogen production from steam reforming in order to evaluate H_2 yield, selectivity to H_2, overall CO_2 emissions, and the energy demand as a function of the kind of fuel and the process variables. This data could serve as a foundation for further examination of fuel-specific reactor and catalyst configurations, which would enable the enhancement of streamlined procedures and may serve as a reference point for comparing outcomes in all studies on the advancement of alternative fuel reforming of interest. In general, the thermodynamic behaviour of these alternative fuels in the steam reforming process are examined, as well as their potential as sustainable options for hydrogen production.

The following sub-sections report a summary of the current knowledge about thermodynamic, process, and catalytic aspects of methane (Section 1.1), methanol (Section 1.2), ethanol (Section 1.3), glycerol (Section 1.4), propane (Section 1.5) and biogas (Section 1.6) steam reforming. Thermodynamic analysis of steam reforming of different fuels was performed, focusing on the comparison of hydrogen yield and energy demand at different operating conditions (pressure, temperature,

and H_2O/fuel ratio). Therefore, the equilibrium composition and hydrogen yield were calculated using the principle of minimizing Gibbs free energy for the following variable ranges: pressure 1–40 bar, temperature 25–1000 °C and water-to-fuel ratio 1–10. In addition, global CO_2 emissions and heat required for each fuel were evaluated under typical operating conditions. The methodology is reported in Section 2, while the equilibrium composition, hydrogen yield and selectivity are reported in Section 3.1. Section 3.2 shows a comparison of the hydrogen yield normalising the water-to-fuel ratio with respect to the number of carbon atoms. In addition, a comparison between thermodynamic and experimental results (data from literature in supplementary materials) is reported in the text. The energy demand and CO_2 footprint are reported in Section 3.3.

1.1. Methane steam reforming

SRM, or natural gas steam reforming, is a well-established technology and currently is the most widely used hydrogen production method [23]. By utilizing methane (CH_4) and steam, the endothermic steam reforming (SR) reaction (1.1) allows the production of H_2 and carbon monoxide (CO). Through the exothermic water-gas shift (WGS) reaction (1.2), the CO can be converted further, resulting in the generation of extra hydrogen and carbon dioxide (CO_2). When these reactions are combined, they form an overall reaction (1.3) that effectively converts methane into carbon dioxide and hydrogen [24].

$$CH_4 + H_2O \leftrightarrow CO + 3H_2 \quad \Delta H = +206.2\frac{kJ}{mol} \tag{1.1}$$

$$CO + H_2O \leftrightarrow CO_2 + H_2 \quad \Delta H = -41.1\frac{kJ}{mol} \tag{1.2}$$

$$CH_4 + 2H_2O \leftrightarrow CO_2 + 4H_2 \quad \Delta H = +164.9\frac{kJ}{mol} \tag{1.3}$$

At 1 bar and below 600 °C, the main reforming reaction (1.1) is highly endothermic and not spontaneous ($\Delta G > 0$). Additionally, the methane molecule requires a high temperature to accomplish high conversion during SRM, has a high C–H bond dissociation energy of 435 kJ/mol, and is relatively stable [25]. This means that the reforming reaction is an energetically demanding process, mandating the provision of an adequate level of external heat and specially designed equipment to carry out the reaction at high temperature and pressure, leading to difficulties in mass and heat transfer [26]. Simultaneously, according to the Le Chatelier's principle, t is advisable to maintain low pressure during the process. The reforming reactions, (1.1) and (1.3), are usually occur within an elevated temperature range of 700–1000 °C, under pressure of 20–35 atm [27,28].

To attain significant conversion and selectivity to hydrogen, the steam reforming reaction necessitates the employment of catalysts. Conventional and commercial SRM typically catalysts consist of nickel on oxide supports, which are usually aluminium or magnesium. Among them, Ni/Al_2O_3 is most commonly used due to its favourable cost-efficiency and elevated activity. Nonetheless, these catalysts often encounter challenges associated with carbon deposition resulting from the Boudouard reaction (1.4) and methane decomposition (1.5), as well as the sintering of Ni particles [24,28].

$$2CO \leftrightarrow C + CO_2 \quad \Delta H = -171.0\frac{kJ}{mol} \tag{1.4}$$

$$CH_4 \leftrightarrow C + 2H_2 \quad \Delta H = +75.0\frac{kJ}{mol} \tag{1.5}$$

Designing enhanced Ni catalysts has received significant attention from the scientific community. In particular, the research is focusing on the modification of promoter, new support materials, and self-supporting of these catalysts. Furthermore, non-Ni-based catalysts such as noble metal (e.g., Ru, Rh) have emerged as viable alternatives, offering high activity and stability in steam reforming. However, the utilization of noble metals is restricted due to their high cost and limited availability, posing challenges for widespread industrial implementation [26,29].

Carbon monoxide levels in the gas mixture resulting from the reforming reaction are typically 5 % or more. To enhance the hydrogen yield and to reduce the content of CO, the produced gas mixture is directed into a water gas shift reactor, where the temperature is kept as low as 200–400 °C [27]. The resultant gas mixture contains primarily 70–75 % hydrogen, with minor amounts of CO (7–10 %), CO_2 (6–14 %) and methane (2–6 %) [23,30].

Current research focuses on developing a highly efficient SRM process and lowering the necessary reaction temperature. In addition, numerous cutting-edge technologies have emerged to enhance steam reforming efficiency while minimizing overall energy consumption. This include dry reforming with carbon dioxide (DRM) [31], partial oxidation (POx), autothermal reforming (ATR), low temperature SMR [32], sorbent enhanced SRM (SE-SRM) [33], chemical looping process (CL-SMR) [34], photocatalytic SRM [35], thermo-photo hybrid SRM [36], plasma SRM [37], and electro-catalytic SRM.

1.2. Methanol steam reforming

Methanol stands out among the alternative fuels due to its highest hydrogen-to-carbon atomic ratio. Containing only one carbon atom, methanol readily reacts with steam at lower temperatures through a process called methanol steam reforming (SRMe) (1.6). This enables the conversion of methanol into a high-purity hydrogen stream while minimizing the formation of carbon [10,38]. The typical operating conditions of the methanol steam reforming are: 1 bar, 250–300 °C, H_2O/Methanol = 1–3. The total reaction network is as follows:

$$CH_3OH + H_2O \leftrightarrow CO_2 + 3H_2 \quad \Delta H = +49.7\frac{kJ}{mol} \tag{1.6}$$

$$CH_3OH \leftrightarrow CO + 2H_2 \quad \Delta H = +90.2\frac{kJ}{mol} \tag{1.7}$$

The most relevant side reactions are methanol decomposition (1.7) and the WGS reaction (1.2) [39]. The decomposition rate of methanol is much lower compared to steam reforming. However, at low water-to-methanol ratio, side reactions are more likely to occur, leading to the production of methane, methane, methyl formate (HCO_2CH_3), dimethyl ether ($(CH_3)_2O$), etc. and other by-products (1.8-1.12) [13].

$$2CH_3OH \leftrightarrow (CH_3)_2O + H_2O \quad \Delta H = -23.0\frac{kJ}{mol} \tag{1.8}$$

$$2CH_3OH \leftrightarrow CH_4 + 2H_2 + CO_2 \quad \Delta H = -66.9\frac{kJ}{mol} \tag{1.9}$$

$$2CH_3OH \leftrightarrow HCO_2CH_3 + 2H_2 \quad \Delta H = +64.4\frac{kJ}{mol} \tag{1.10}$$

$$CH_3OH \leftrightarrow CH_2O + H_2 \quad \Delta H = +84.7\frac{kJ}{mol} \tag{1.11}$$

$$CH_3OH \leftrightarrow C + H_2O \quad \Delta H = +159.52\frac{kJ}{mol} \tag{1.12}$$

The resulting gas typically contains around 75 % H_2, 25 % CO_2, and 1 % CO [40,41]. Enhancing various components of the SRMe system, including reactors, catalysts, and separation membranes, is crucial for optimizing the efficient production of hydrogen [40]. The separation of hydrogen from the product mixture plays a significant role in overall costs. Membrane reactors offer higher efficiency compared to conventional reactors by combining the reaction and separation of hydrogen and other by-products in a single unit, eliminating the need for additional processing steps. Thus, membrane reactors are cost-efficient due

to the bypassing of the WGS reaction [13]. However, packed bed reactors are more commonly used in practical applications due to design challenges and the higher production costs associated with membrane reactors.

The efficiency of SRMe process relies heavily on the catalyst employed. Copper-based catalysts and group VIII metal-based catalysts, including Ni, Pt, Pd, Ru, and Rh, are commonly employed in this process. These catalysts are typically supported on oxide materials with a large surface area, such as Al_2O_3 [40]. Copper-based catalysts offer high activity and selectivity, but they can experience catalytic deactivation due to factors like thermal sintering, coke deposits, and changes in oxidation state [42]. The catalytic performance is affected by both metal component and support material. Promoters, such as acidic oxides or alkali metals, can eliminate undesired compounds formed during the reaction [13].

1.3. Ethanol steam reforming

During the process of steam reforming of ethanol (SRE) process, the primary reactions result in the production of CO_2 and H_2 (1.13). Additionally, various carbonaceous by-products such as CH_4, CO, acetaldehyde (CH_3CHO), and ethylene (C_2H_4), are formed. Side reactions, including ethanol dehydrogenation (1.14) and ethanol decomposition (1.15), as well as the WGS (1.2) to form H_2 [10]:

$$C_2H_5OH + 3H_2O \leftrightarrow 2CO_2 + 6H_2 \quad \Delta H = +173.5\frac{kJ}{mol} \tag{1.13}$$

$$C_2H_5OH \leftrightarrow CH_3CHO + H_2 \quad \Delta H = +68.9\frac{kJ}{mol} \tag{1.14}$$

$$C_2H_5OH \leftrightarrow CH_4 + CO + H_2 \quad \Delta H = +49.0\frac{kJ}{mol} \tag{1.15}$$

$$CH_3CHO \leftrightarrow CH_4 + CO \quad \Delta H = -19.3\frac{kJ}{mol} \tag{1.16}$$

$$CH_3CHO + H_2O \leftrightarrow 2CO + 3H_2 \quad \Delta H = +186.8\frac{kJ}{mol} \tag{1.17}$$

$$CH_4 + CO_2 \leftrightarrow 2CO + 2H_2 \quad \Delta H = +54.0\ \text{kJ/mol} \tag{1.18}$$

$$C_2H_5OH \leftrightarrow C_2H_4 + H_2O \quad \Delta H = +45.5\frac{kJ}{mol} \tag{1.19}$$

$$2CH_3CHO \leftrightarrow CH_3COCH_3 + CO + H_2 \quad \Delta H = +4.1\frac{kJ}{mol} \tag{1.20}$$

$$C_2H_4 \rightarrow Polymers \rightarrow Coke \tag{1.21}$$

Dehydrogenation (1.14) is a crucial step in H_2 production and is enhanced by high temperature. Acetaldehyde steam reforming (1.17) and WGS (1.2) reactions proceed sequentially. Ethanol decomposition (1.15), SRM (1.1) and methane dry reforming (1.18), are also advantageous at high temperature [43]. Several side reactions take place, including dehydration of ethanol (1.18), decomposition of acetaldehyde (1.16), acetone formation (1.20) and coke formations (methane decomposition (1.5), Boudouard reaction (1.4), polymerization of ethylene (1.21)) [44]. An appropriate range of operating conditions for SRE are: 1 bar, 250–800 °C, H_2O/Ethanol = 3–5 [45].

SRE commonly employs Co-based and Ni-based catalysts due to their cost-effectiveness and strong ability to break to C–C bonds. These catalysts are usually spread inside a matrix like Al_2O_3, SiO_2, ZrO_2, MgO and others. However, they do have some drawbacks, such as deactivation caused by carbon deposits and the formation of methane as a byproduct. To mitigate these issues in ESR, two approaches have been suggested: incorporating a second element and utilizing alternative catalytic supports. For example, introducing basic oxides (MgO, Na_2O, CaO) in the catalytic support (e.g. alumina), helps neutralizing its acidity, inhibiting ethanol dehydration. On the other hand, the utilization of a redox-active promoter (CeO_2) directly aids in the coke oxidation. Introducing a secondary metal into the Ni-based catalyst, such as Au, Cu, Fe, or Co, can lead to the formation of different structures that exhibit enhanced resistance to carbon deposition due to the reduced diffusion of carbon atoms in metal nanoparticles [44].

To enhance overall energy efficiency, various reactor configurations and structured catalysts have been employed to improve heat and mass transfer. A combined system of reaction and separation was found to be effective to increase both hydrogen purity and equilibrium conversion. Extensive research has been conducted both on membrane reactors and CO_2 sorption enhancement by SRE using a CO_2 absorbent for in situ CO_2 separation [44].

1.4. Glycerol steam reforming

On of the many applications for glycerol is it usage as a source of hydrogen via the steam reforming process. The overall reaction for the steam reforming of glycerol (SRG) (1.22) is shown in the following equation [17]:

$$C_3H_8O_3 + 3H_2O \leftrightarrow 7H_2 + 3CO_2 \quad \Delta H = +127.7\frac{kJ}{mol} \tag{1.22}$$

As for the other fuels, the WGS reaction (1.2) takes place and leads to the production of extra hydrogen. According to several studies [10,17,46–48] there are secondary reactions such as the decomposition of glycerol (1.23) and CO methanation (1.24) and CO_2 methanation (1.25). Methanation may take place at low temperatures, with part of the hydrogen produced reversibly mixing with the oxygenated molecules in the system to form methane. At high temperature, coke formation may occur due to the Boudouard reaction (1.4), methane decomposition (1.5), and hydrogenation of CO (1.26) and CO_2 (1.27).

$$C_3H_8O_3 \leftrightarrow 4H_2 + 3CO \quad \Delta H = +253.50\frac{kJ}{mol} \tag{1.23}$$

$$CO + 3H_2 \leftrightarrow CH_4 + H_2O \quad \Delta H = -206.2\frac{\text{kJ}}{mol} \tag{1.24}$$

$$CO_2 + 4H_2 \leftrightarrow CH_4 + 2H_2O \quad \Delta H = -164.6\frac{kJ}{mol} \tag{1.25}$$

$$CO + H_2 \leftrightarrow C + H_2O \quad \Delta H = -131.3\frac{kJ}{mol} \tag{1.26}$$

$$CO_2 + 2H_2 \leftrightarrow C + 2H_2O \quad \Delta H = -90.1\frac{kJ}{mol} \tag{1.27}$$

Given that the ratio of the hydrogen to glycerol molecules is 7:1, producing hydrogen from glycerol may be appealing. According to the literature, the best results are achieved at temperature between 525 and 725 °C. The commonly used pressure is around 1 atm. Even at higher temperatures, the H_2 yield increases more slowly at ratios above 9. The required volume of water shouldn't be excessive due to the high costs involved with evaporation, so the optimal amount of steam depends on the adopted catalyst and the operating conditions, especially temperature and pressure [46–48].

As mentioned above, the complex reaction network of SRG causes the production of unwanted by-products. In order to ensure the sustainable use of glycerol, there is a high demand for efficient catalysts that can selectively produce H_2 production at low reaction temperatures [49]. Palladium (Pd), ruthenium (Ru), iridium (Ir), rhodium (Rh) and platinum (Pt) display high catalytic performance and excellent physicochemical features. However, their limited availability and high price make them uneconomical. Nickel (Ni), cobalt (Co) and copper (Cu), among other transition metals, provide affordable alternatives and are widely available. The development of innovative catalysts using the combination of several metals has been the focus of recent research to

Table 1
Summary of the operating temperature, water-to-fuel ratio (n), pressure, and main catalysts used in commercial applications for the different fuel investigated for steam reforming process.

Fuel	T_R, °C	n	P, bar	Catalysts	Ref
Methane	700–1200	3–6	20–35	Ni/Al_2O_3	[27,28]
Biogas	800–900	0.5–2.5	1–7	Ni/Al_2O_3 Ni/SiC Ni/ZrO_2	[21]
Propane	800–900	3	20	Ni/Al_2O_3 Rh/Al_2O_3 $Ru/CeO_2–ZrO_2$	[18,61]
Methanol	250–400	1–3	1	$Cu/ZnO/Al_2O_3$	[39,42]
Ethanol	250–800	3–5	1	Ni/Al_2O_3 Co/Al_2O_3	[44,45]
Glycerol	500–900	3–10	1	Ni/Al_2O_3 $Ni/SiO_2–Al_2O_3$	[47,64]

obtain improved product selectivity and superior catalytic activity: due to enhanced metal dispersion, a bimetallic Ni/noble metal catalyst increases carbon resistance and has good catalytic activity; Ni with other transition metals, namely Cu, Fe and Co leads to different catalytic performances based on their individual nature. Due to its large specific surface area and thermal stability, alumina is used as the primary catalytic support. However, it is vulnerable to deactivation brought on by catalyst sintering and carbon adsorption. The addition of alkali elements can improve the stability of catalysts and somewhat lessen their acidity. Additionally, this basic nature encourages the water dissociation, methane reforming, and water-gas shift reaction [16,50].

In addition to conventional steam reforming of glycerol, sorption-assisted steam reforming [51,52], chemical looping reforming [53], aqueous phase reforming [54], supercritical steam reforming [55], and photocatalytic reforming [56] has also been investigated.

1.5. Propane steam reforming

The simultaneous occurrence of propane steam reforming (SRP) (1.28) and the WGS (1.2) is reported as the overall SRP (1.29) [57]:

$$C_3H_8 + 3H_2O \leftrightarrow 3CO + 7H_2 \quad \Delta H = +499.0\frac{kJ}{mol} \tag{1.28}$$

$$C_3H_8 + 6H_2O \leftrightarrow 3CO_2 + 10H_2 \quad \Delta H = +373.7\frac{kJ}{mol} \tag{1.29}$$

By-products such as methane and ethylene may also be produced under reaction conditions via the propane decomposition reactions (1.30), CO or CO_2 methanation (1.24, 1.25) [58].

$$C_3H_8 \leftrightarrow C_2H_4 + CH_4 \quad \Delta H = +81.0\frac{kJ}{mol} \tag{1.30}$$

$$C_3H_8 \leftrightarrow C_3H_6 + H_2 \quad \Delta H = +125.0\frac{kJ}{mol} \tag{1.31}$$

Efficient H_2 production in SRP research has primarily focused on the development of catalyst. Nickel-based catalysts have been extensively studied for efficient H_2 production due to their low cost, however they face issues such as particle sintering, and carbon deposition caused by the decomposition of C_2H_4 and CH_4 (1.21, 1.5) and/or the Boudouard reaction (1.4). Current research focuses on developing novel catalyst formulations capable of selectively converting C_3H_8 to H_2 while resisting coke formation and particle agglomeration. By adjusting catalyst synthesis parameters such as preparation procedure, pH, temperature, and ageing time, the size of Ni nanoparticles can be controlled, and carbon deposition can be avoided by enhancing Ni-based catalysts with alkali metals or lanthanides [58]. Alkali metal oxides such as K_2O and CaO have demonstrated improved resistance to coking by enhancing carbon gasification, but at the expense of catalytic activity. Addition of small amounts of molybdenum or tungsten (0.5 wt% MoO_3 or WO_3) can enhance coking resistance without sacrificing catalytic activity. Lanthanides, on the other hand, show promise as promoters since they may prevent the formation of coke without losing catalytic activity [59,60]. Conversely, partial or complete substitution of Ni with noble metals (Rh, Pt, Ru, Rh) has resulted in catalytic materials with excellent properties and improved catalyst durability, but higher costs [58,61].

In the SRP industrial practice, propane or LPG may be fed first to a pre-reformer, operating at 450–500 °C, in which all hydrocarbon

Table 2
Chemical species considered in the equilibrium system for each fuel.

Fuel	Species	Ref.
Methane	CH_4, CO_2, CO, H_2, H_2O, C	[1]
Biogas	CH_4, CO_2, CO, H_2, H_2O, C	[63]
Propane	Propane, ethylene, propylene, CH_4, CO_2, CO, H_2, H_2O and C	[19]
Methanol	Methanol, methyl formate, dimethyl ether, formaldehyde, CH_4, CO_2, CO, H_2, H_2O and C	[13]
Ethanol	Ethanol, acetaldehyde, ethylene, acetone, ethane, acetic acid, CH_4, CO_2, CO, H_2, H_2O and C	[44,71]
Glycerol	Glycerol, acetaldehyde, ethylene, ethanol, methanol, ethane, propylene, acetone, acrolein, formaldehyde, allyl alcohol, propionaldehyde, acetic acid, CH_4, CO_2, CO, H_2, H_2O and C	[71]

Table 3
Overall steam reforming reactions and stoichiometric water-to-fuel ratio (n_{stoic}).

Fuel	Global steam reforming reaction	n_{stoic}
Methane	$CH_4 + 2H_2O \leftrightarrows CO_2 + 4H_2$	2
Biogas	$CH_4 + 2H_2O \leftrightarrows CO_2 + 4H_2$	2
Propane	$C_3H_8 + 6H_2O \leftrightarrows 3CO_2 + 10H_2$	6
Methanol	$CH_3OH + H_2O \leftrightarrows CO_2 + 3H_2$	1
Ethanol	$C_2H_5OH + 3H_2O \leftrightarrows 2CO_2 + 6H_2$	3
Glycerol	$C_3H_8O_3 + 3H_2O \leftrightarrows 3CO_2 + 7H_2$	3

Table 4
Operating conditions for the calculation of the heat duty required at reactor, Q_R, and at heat exchanger, Q_{HE}.

Fuel	T_{IN}, °C	T_R, °C	n	P, bar
Methane	250	600–1200	3	20
Biogas	250	600–1200	2.5	7
Propane	250	600–1200	3	20
Methanol	125	250–600	3	1
Ethanol	170	350–800	3	1
Glycerol	300	500–1000	7	1

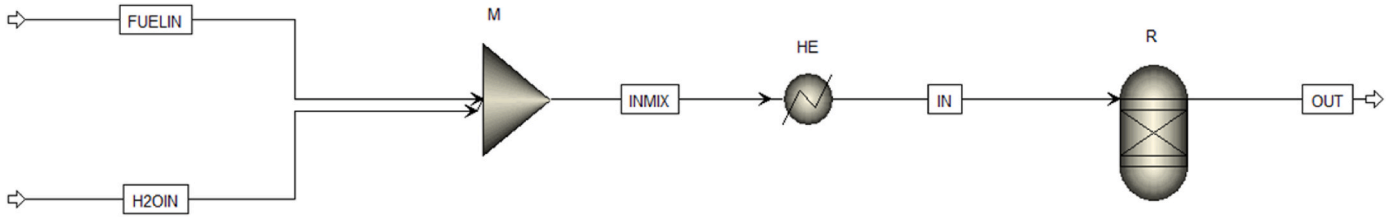

Fig. 1. Process Flowsheet implemented in AspenPlus®.

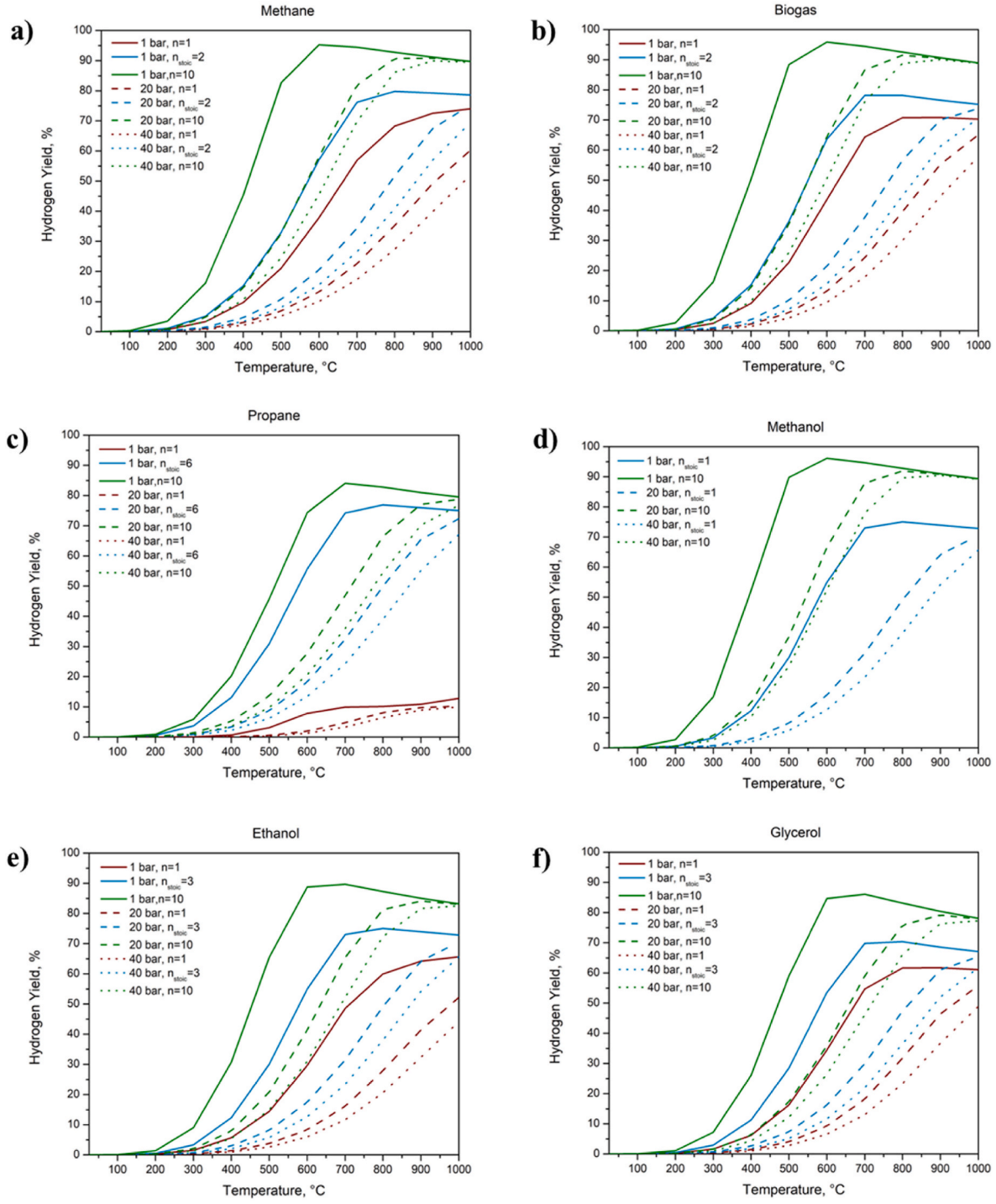

Fig. 2. Hydrogen yield as a function of temperature parametric in the pressure (1 bar solid, 20 bar dashed, 40 bar dotted lines) and in the water-to-fuel feed ratio (n = 1 red, n = n_{stoic} blue and n = 10 green lines) for the steam reforming of: a) methane, b) biogas, c) propane, d) methanol, e) ethanol and f) glycerol. (For interpretation of the references to colour in this figure legend, the reader is referred to the Web version of this article.)

heavier than methane are completely converted to C1 components; than a methane-rich gas which is introduced to steam reformer operating at higher temperature (850–900 °C) [18].

1.6. Biogas steam reforming

While the establishment of commercial usage for dry methane reforming (DRM) alone remains pending, the industrial application of combined dry and steam reforming techniques has been in practice for several years. Several examples of this include the CALCOR process (Caloric GmbH) and the SPARG process (Haldor Topse), both of which are based on the DRM reaction. There are two commercial technologies that alter the H_2/CO ratio, operate under milder conditions, and combine SRM or POx with DRM [62]. By combining steam and dry reforming of methane, commonly referred to as steam biogas reforming (SMB) or bi-reforming, an efficient method for producing syngas is achieved, while also reducing net CO_2 emissions compared to the steam reforming process. However, for the bi-reforming process to occur in the presence of significant amounts of O_2, it must be removed from the biogas [63].

Table 5
Maximum hydrogen yield and corresponding operating conditions.

P, bar	n	Methane		Biogas		Propane		Methanol		Ethanol		Glycerol	
		T, °C	Y_{H_2}, %	T, °C	Y_{H_2}, %	T, °C	Y_{H_2}, %	T, °C	Y_{H_2}, %	T, °C	Y_{H_2}, %	T, °C	Y_{H_2}, %
1	1	1000	73.97	900	70.80	1000	12.78	800	75.04	1000	65.65	900	61.71
	Stoic	800	79.76	700	78.16	800	76.86	–	–	800	75.04	800	70.31
	10	600	95.26	600	95.85	700	84.03	600	96.10	700	89.66	700	86.05
20	1	1000	60.24	1000	65.08	1000	10.21	1000	70.47	1000	52.19	1000	55.87
	Stoic	1000	75.31	1000	73.83	1000	72.36	–	–	1000	70.47	1000	65.41
	10	900	90.83	800	91.47	1000	78.76	800	91.92	900	84.08	900	79.18
40	1	1000	51.99	1000	57.81	1000	9.92	1000	65.67	1000	44.17	1000	48.88
	Stoic	1000	69.46	1000	70.57	1000	67.13	–	–	1000	65.67	1000	61.75
	10	900	89.97	900	90.05	1000	76.79	900	90.46	1000	82.49	1000	77.26

According to the literature [21,22,63], the main reactions involved in the biogas reforming are methane dry reforming (1.32), SRM (1.1) and WGS (1.2). Thus, both CO_2 and H_2O play the role of oxidants. The coexistence of CO_2 and H_2O influences the WGS equilibrium [22]. Under reforming conditions, coke formation may occur due to methane decomposition (1.5) and Boudouard reaction (1.4).

$$CH_4 + 3CO_2 \leftrightarrow 2CO + 2H_2 \quad \Delta H = +247.0\frac{kJ}{mol} \tag{1.32}$$

The biogas reforming process typically occurs within temperatures of 800–850 °C and pressure of 1–7 bar. The CH_4 to CO_2 ratio and CH_4 to H_2O ratio generally fall between 1–3 and 0.5–1.5, respectively. The conversion of CH_4 and CO_2 is generally over 61 % and 33 %, respectively [21]. Therefore, the main challenges entail achieving higher reactant conversion and catalyst deactivation. Mainly, Ni-based catalysts with various supports such as Al_2O_3, SiC, and ZrO_2 are used, but these conventional catalysts tend to deactivate due to coke formation and metal sintering. Nevertheless, the formation of coke can be significantly minimised by using precious metal-based catalysts or Ni-based materials doped with rare earths (e.g. Ru, Rh and Ni–Ce) [21,63].

Table 1 summarizes the commercial operating conditions and the main catalysts for steam reforming process for each fuel investigated.

2. Modelling and simulation methodology

2.1. Thermodynamic analysis

The Gibbs free energy minimisation technique was applied to obtain the equilibrium compositions for each gas species within each reacting system, using steam reforming of methane, biogas, propane, methanol, ethanol, and glycerol. The equilibrium gas composition of each reacting system can be calculated by minimizing the total Gibbs free energy using a non-stochiometric approach, where it is not necessary to specify a set of reactions taking place in the system. The total Gibbs free energy of a system (G^t) is composed by the sum of the total moles of each component (n_i) in the system multiplied by the component chemical potential (μ_i):

$$G^t = \sum_{i=1}^{N} n_i \mu_i \tag{2.1}$$

Under equilibrium conditions, the total Gibbs energy of the system decreases until it reaches a minimum, where its differential is zero. Consequently, the equilibrium state of any reaction system can be obtained using the Gibbs free energy minimisation function [65–69]. The equilibrium calculations were performed with AspenPlus® using Gibbs energy minimisation with the RGIBBS reactor model [19]. In RGIBBS, phase equilibrium and chemical equilibrium were chosen as calculation options. The property method chosen for the model, Peng-Robinson, is commonly used for thermodynamic analysis of polar and non-polar mixtures and for hydrocarbons and light gases [70]. As shown in Fig. 1, the fuel and water streams were mixed in a mixer unit (M) upstream of the reactor and fed into a heat exchanger (HE) to bring the reactant mixture to reactor (R) operating conditions.

The procedure for minimizing the Gibbs free energy takes into account all possible reactions within the thermodynamic reaction system in which the species in equilibrium must be defined. The equilibrium system consists of the following gas species CH_4, CO_2, CO, H_2, H_2O and C for each fuel. In addition, other species have been added to the equilibrium system based on reaction pathways found in the literature, which are summarised in Table 2.

For each fuel, the effect of temperature, pressure and water-to-fuel ratio was investigated. Particularly, the temperature was varied between 25 °C and 1000 °C, the pressure in the range of 1–40 bar, and the water-to-fuel ratio (denoted as n) in the range of 1–10. In particular, the water-to-fuel ratio has been set as of 1, the stoichiometric value (n_{stoic}) for the total steam reforming (reported in Table 3) and 10. In the case of biogas, the CH_4/CO_2 fed ratio was kept unchanged and equal to 3/1, while n (H_2O/CH_4) was varied in the range 1–10.

2.2. Hydrogen yield, fuel conversion and selectivity

The defined criteria for evaluate the steam reforming system effectiveness include the equilibrium conversions of the various fuel, X_{eq}, the hydrogen yield, Y_{H_2}, and the selectivity to product, S_i, were defined as follows:

$$X_{eq} = \frac{F_{fuel,in} - F_{fuel,out}}{F_{fuel,in}} \bullet 100 \tag{2.2}$$

$$Y_{H_2} = \frac{F_{H_2,out}}{\nu_{H_2} \bullet F_{fuel,in}} \bullet 100 \tag{2.3}$$

$$S_i = \frac{F_{i,out}}{\sum_j F_{j,out}} \bullet 100 \tag{2.4}$$

Where $F_{fuel,in}$ and $F_{fuel,out}$ are the inlet and outlet molar flow rates, respectively, $F_{H_2,out}$ is outlet hydrogen molar flow rate and, $F_{j,out}$ are the molar flow rates of the product leaving the reactor excluding unconverted fuel and steam. ν_{H_2} is the stoichiometric coefficient of hydrogen in the overall steam reforming reaction of the fuel (Table 3).

In addition, a comparison of the hydrogen yields of the different fuels was made at equal water-to-C ratio (Equation (2.5)). In particular, the water-to-C ratio was set to 3, the typical water-to-methane ratio in commercial SRMs. As demonstrated in Eq. (2.6), for each fuel ($C_xH_yO_z$) the hydrogen yield was calculated for a water-to-fuel ratio of $x \bullet 3$, so that a comparison of the yield for the same water-to-C atom ratio could be made. The results are reported in Section 3.2.

$$\frac{H_2O}{C} = 3 \tag{2.5}$$

$$\frac{H_2O}{x \bullet C_xH_yO_z} = 3 \tag{2.6}$$

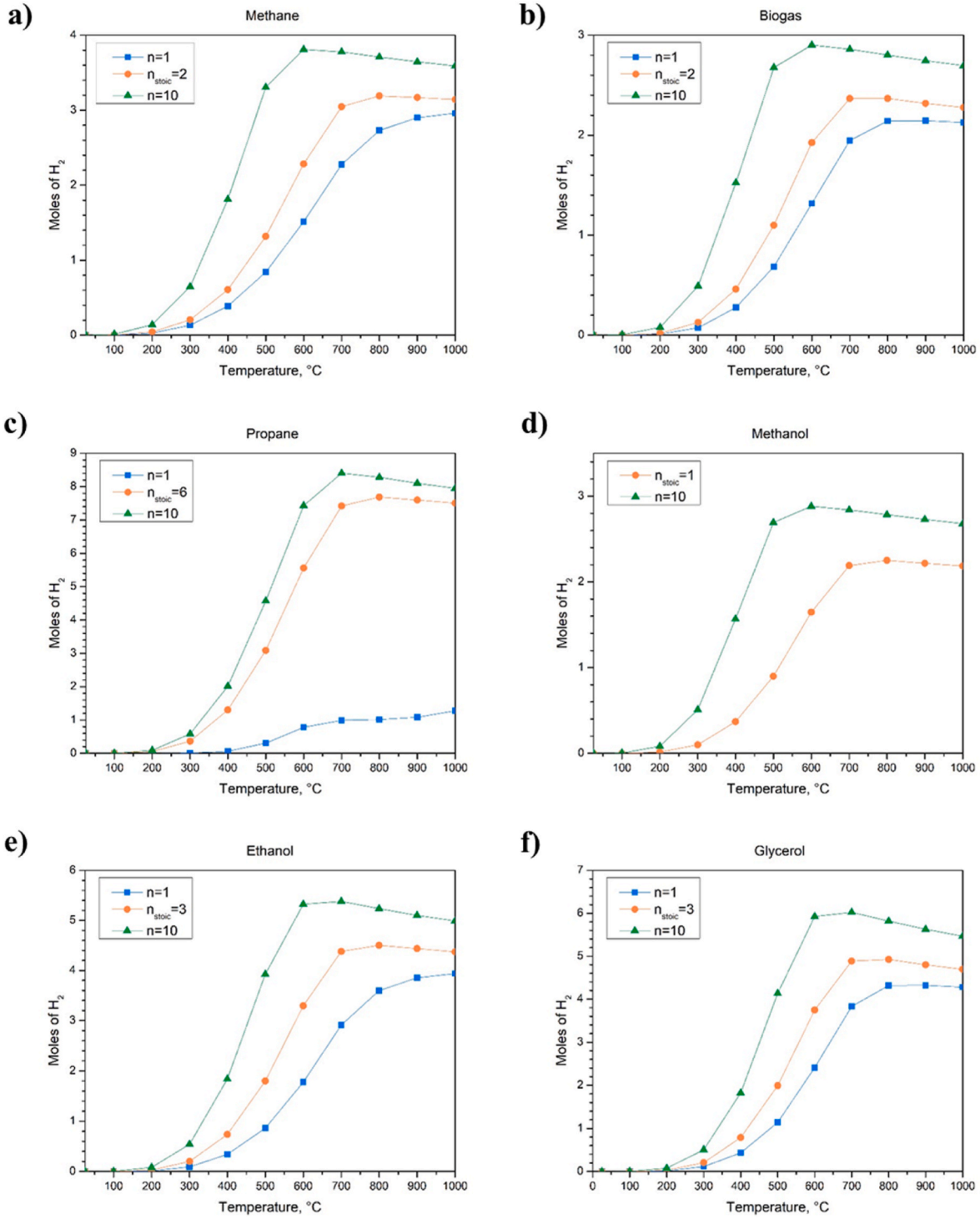

Fig. 3. Moles of hydrogen as a function of temperature at different water-to-fuel (n) ratio at P = 1 bar for steam reforming of: a) methane, b) biogas, c) propane, d) methanol, e) ethanol, and f) glycerol.

2.3. Energy demand and CO_2 footprint

The heat duty required at reactor, Q_R, and at heat exchanger, Q_{HE}, was estimated by varying the reactor operating temperature, T_R and setting the pressure, P, and inlet temperature, T_{IN}, based on literature (Table 1). The fixed value of P and T_{IN} and the range of T_R are reported in Table 4.

Through the energy balance at the reactor, CO_2 emissions per moles of hydrogen produced (m_{CO_2}/n_{H_2}) associated to the combustion flue gases was calculated, assuming that the auxiliary stream were consisted of methane and air in stoichiometric conditions. In Sections 3.2 and 3.3, the results of the heat analysis are presented.

3. Results and discussions

3.1. Equilibrium product composition, hydrogen yield and selectivity

The simulation analysed the varying pressures, temperatures, and

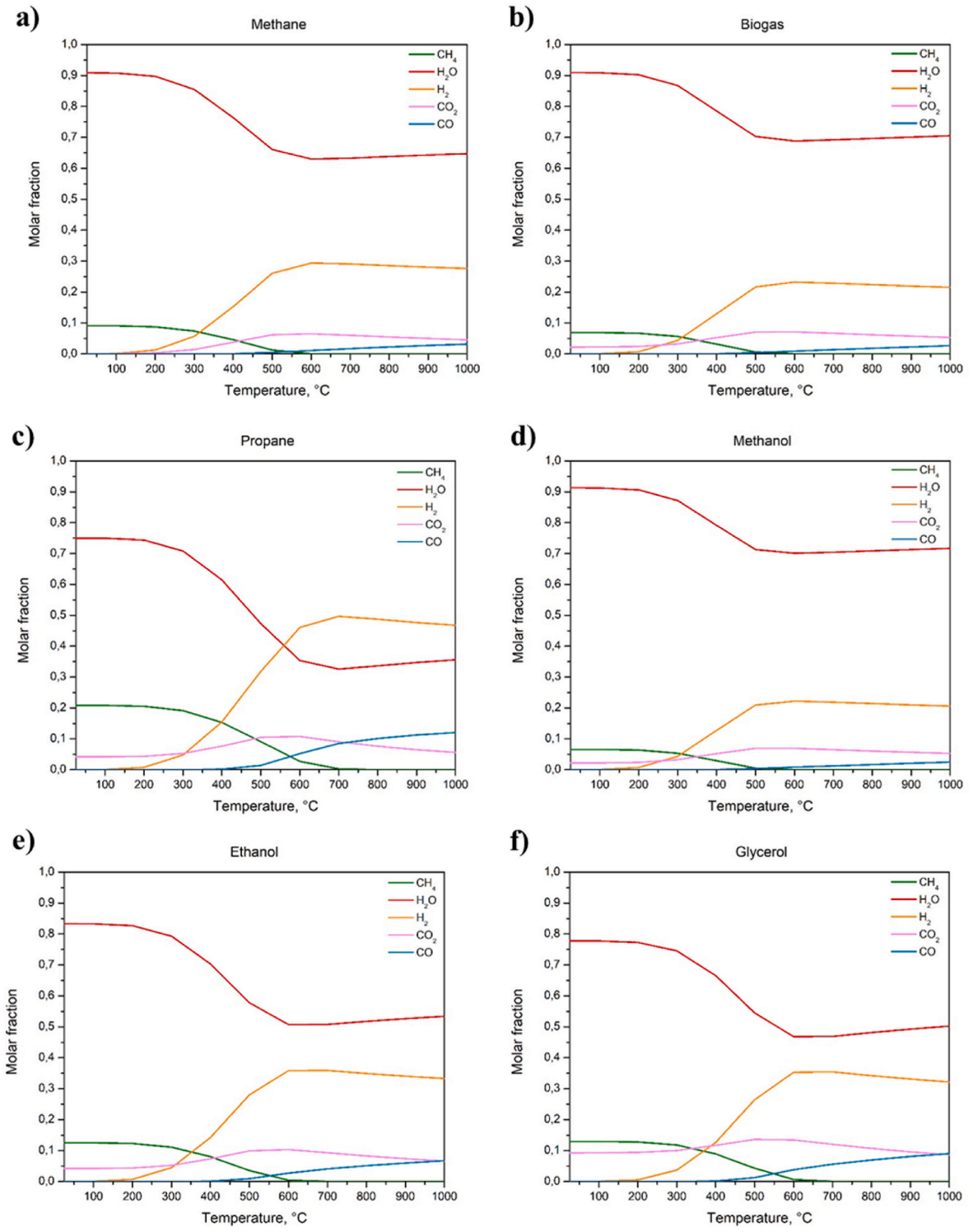

Fig. 4. Molar fraction vs temperature at P = 1 bar and water-to-fuel ratio (n) equal to for steam reforming of: a) methane, b) biogas, c) propane, d) methanol, e) ethanol and f) glycerol.

water-to-fuel ratios to determine the equilibrium composition of hydrogen and other resulting products. The thermodynamic analysis considered all possible reactions in the system consisting of the gases listed in Table 2. However, it was found that only CH_4, CO_2, CO, H_2 and H_2O were present in the system under the selected operating conditions. From the perspective of thermodynamics, methane is the most stable hydrocarbon for the Francis diagram [65], so the main reaction is the SRM. In addition, the conversion of all the investigated fuels in the temperature, pressure, and water-to-fuel ratio ranges investigated was always above 99.99 %, so that complete conversion can be assumed.

Fig. 2 illustrates the relationship between hydrogen yield, Y_{H_2}, and temperature, parametric in the pressure and in the water-fuel ratio. The hydrogen yield declines as the pressure rises, but it increases as the temperature rises, holding the water-fuel ratio constant (as denoted by the same line colour in Fig. 2). This outcome is expected because the steam reforming reaction proceeds with increasing number of moles and

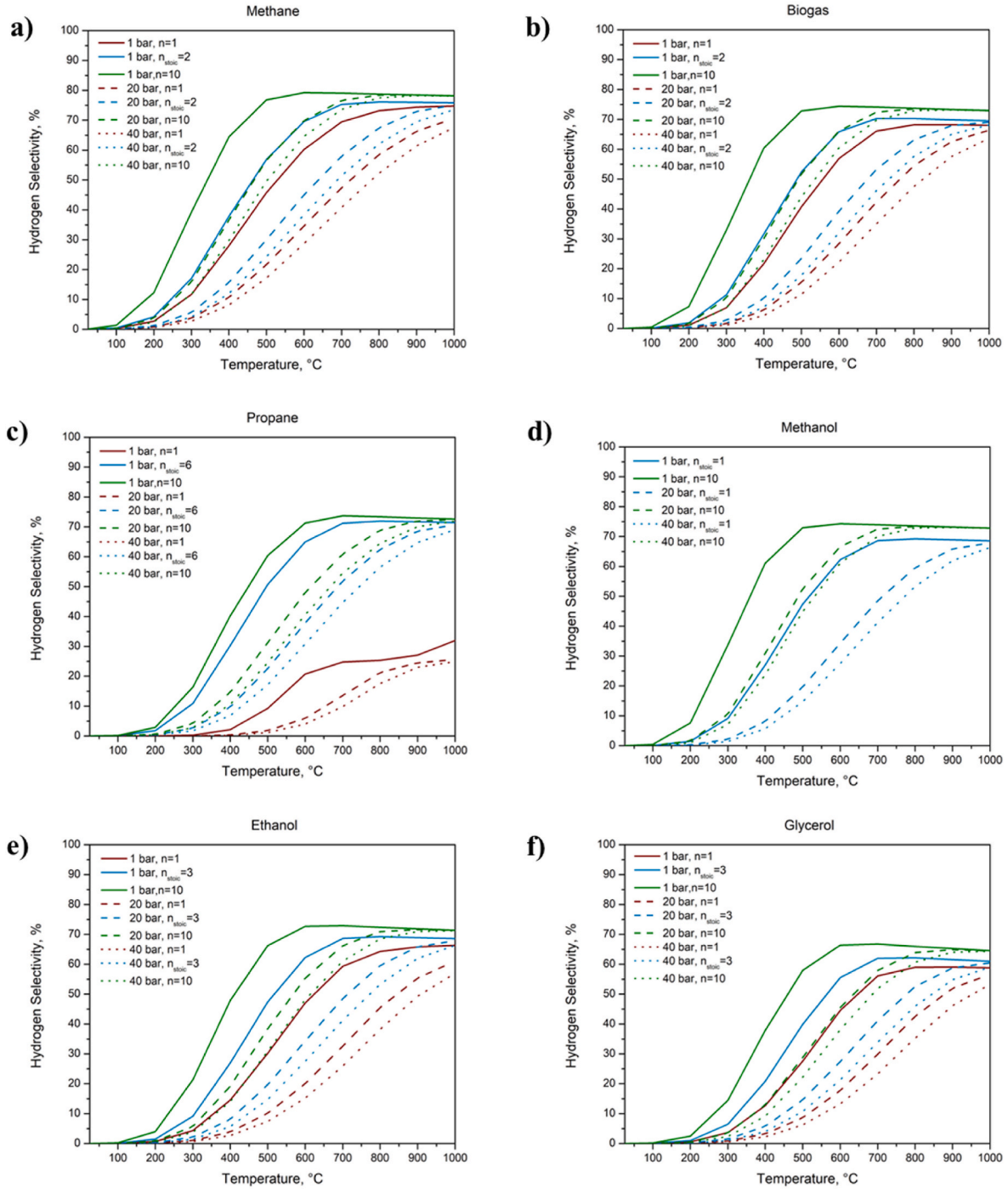

Fig. 5. Selectivity to Hydrogen as a function of temperature parametric in the pressure (1 bar solid, 20 bar dashed, 40 bar dotted lines) and in the water-to-fuel feed ratio (n = 1 red, n = n_{stoic} blue and n = 10 green lines) for steam reforming of: a) methane, b) biogas, c) propane, d) methanol, e) ethanol and f) glycerol. (For interpretation of the references to colour in this figure legend, the reader is referred to the Web version of this article.)

is an endothermic reaction that is favoured at temperature higher than $T_{\Delta G^\circ=0}$. If the water-to-fuel ratio is increased at the same pressure (same lines type in Fig. 2), the fuel is completely consumed, as it is the limiting reactant, and the yield increases. Thus, an excess of water promotes thermodynamic equilibrium, increases the total number of moles produced and promotes gasification. With $n > 10$, on the other hand, the reactor would have to be considerably enlarged, resulting in greater heat per mole of reacting mixture.

This confirms that at low pressure and high water-to-fuel ratio, the maximum yield given in Table 5 is achieved at lower temperatures and under thermodynamically favourable conditions. For example, Table 5 shows that at fixed pressure of 1 bar, for methane the maximum hydrogen yield occurs at 1000 °C for $n = 1$, whereas for $n = 10$ at 600 °C. This behaviour is visible for all the other fuels, in particular the maximum hydrogen yield goes from 900 °C to 600 °C for biogas, from 1000 °C to 700 °C for propane, from 800 °C to 600 °C for methanol, from 1000 °C to 700 °C for ethanol, and from 900 °C to 700 °C for glycerol increasing n from 1 to 10 at 1 bar. The same trend is visible by setting n and decreasing pressure. For example, the temperature at which the maximum hydrogen yield is achieved is reduced from 900 °C to 600 °C for methane, biogas, and methanol, and from 1000 °C to 700 °C for propane, ethanol, and glycerol, by reducing the pressure from 40 to 1

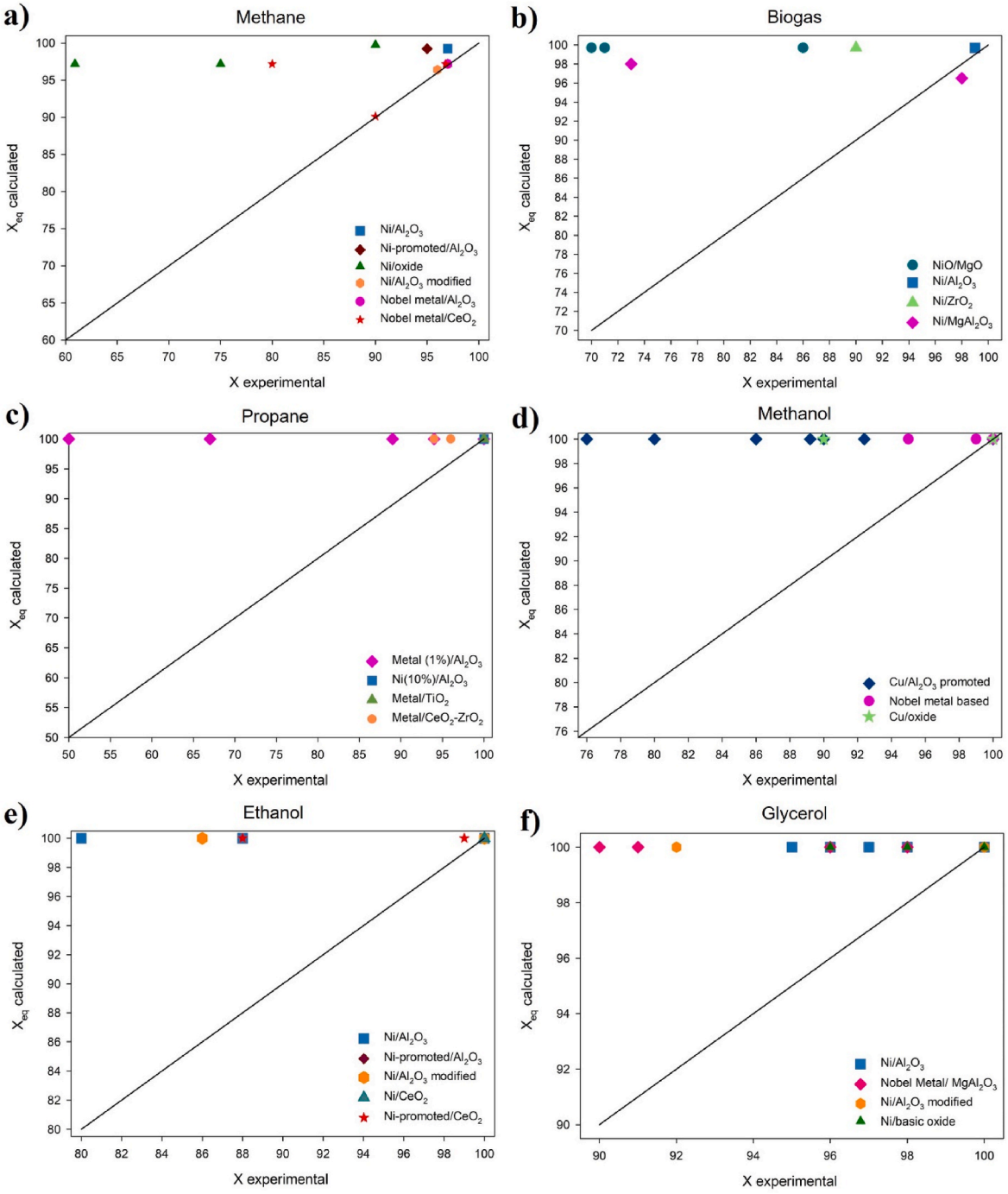

Fig. 6. Parity plot for equilibrium and experimental (Table S2) conversion for steam reforming of: a) methane, b) biogas, c) propane, d) methanol, e) ethanol and f) glycerol.

bar for $n = 10$.

The graph depicted in Fig. 2 demonstrates a non-linear pattern in the relationship between temperature and hydrogen yield. Initially, the yield increases until it reaches a maximum value, after which it declines. This trend is particularly observable at high water-to-fuel ratios and low pressure, i.e. at the most thermodynamically favourable conditions. However, it also present for the stoichiometric condition. This behaviour can be easily understood by looking at the moles of hydrogen produced at equilibrium conditions as well as the equilibrium gas composition.

In Fig. 3, the molar amount of hydrogen produced at 1 bar is shown, parametric in *n*. As expected, a reduction of hydrogen yield is observed as a result of the reduction of produced hydrogen at high temperature and at the highest water-to-fuel ratio ($n = 10$, green line). Fig. 4 shows the molar fractions of the product stream at $P = 1$ bar and $n = 10$ as an example of the equilibrium composition. The other data relative to the equilibrium composition at pressure of 1, 20 and 40 bar and at water-to-fuel ratio of 1, the stoichiometric value for the total steam reforming n_{stoic} (Table 3), and 10 are given in Table S1 for methane, biogas, propane, methanol, ethanol, and glycerol, respectively.

Fig. 4 shows that at high temperature the molar fractions of CO_2 and H_2 decrease, while those of H_2O and CO increase, indicating the occurrence of the rWGS reaction, according to Refs. [19,38,49,67,72]. rWGS is an endothermic reaction unaffected by pressure variations. It takes place at high temperatures and is favoured by a high water-to-fuel

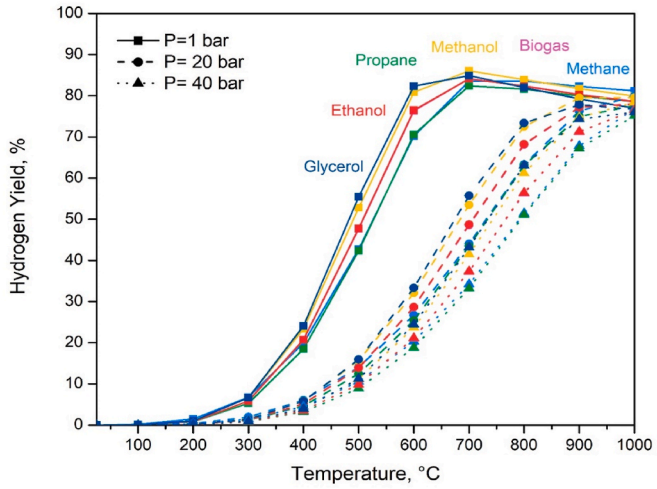

Fig. 7. Hydrogen yield vs temperature parametric in pressure (solid, dashed, dotted lines) for water-to-C ratio equals to 3.

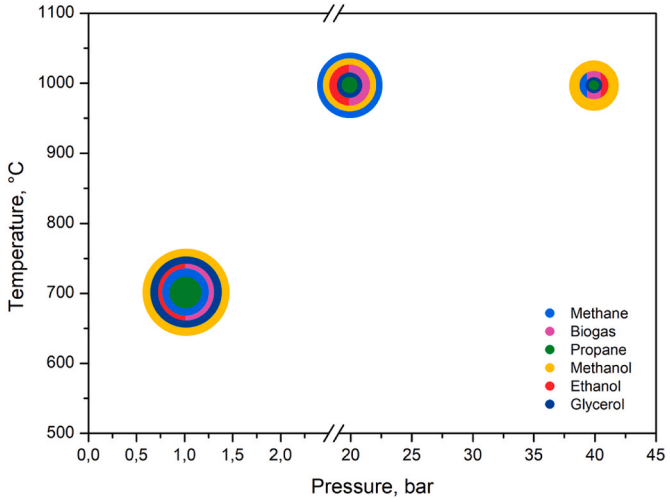

Fig. 8. Diagram of maximum hydrogen yield achieved by methane, biogas, propane, methanol, ethanol, and glycerol at 700 °C and 1 bar, 1000 °C and 20 bar, 1000 °C and 40 bar for fixed water-to-C ratio equals to 3.

ratio, since the H_2/CO_2 ratio is greater. Steam reforming processes aim to produce syngas; however, methane is a common product that competes with H_2. According to data presented in Table S1, exhibits stability at lower temperatures, but its concentration sharply decreases as temperature rises. The molar fraction of methane decreases with increasing temperature and water-to-fuel ratio, while higher pressure favours the formation of CH_4. This trend is due to the SRM reaction, which produces CO or CO_2 and H_2, as given in equations (1.1) and (1.3). At high water-to-fuel ratios ($n = 10$) and high temperatures (>700 °C), methane is consumed by these reactions, while at lower temperatures methane formation is due to the methanation reaction (1.24) and (1.25). CO and CO_2, classified as impurities, do not compete with H_2. The molar fraction of CO increases with temperature but decreases with higher values of n and pressure. CO_2 shows a maximum at a fuel-specific temperature. This behaviour can be attributed to rWGS.

The selectivity to H_2 is shown in Fig. 5. As mentioned above, steam reforming reactions are generally favoured at high temperature, low pressures, and a high water-to-fuel ratio. In fact, selectivity increases with temperature for any value of pressure and n. As n increases (curves at the same pressure with the same shape) and pressure decreases (curves at fixed n with the same colour), selectivity increases. The selectivity to H_2 and CO (Figure S2) increases at higher temperature, while the selectivity to CO_2 (Figure S1) decreases. At high temperatures (>600 °C), rWGS is favoured, leading to an increase in selectivity to CO and a decrease in selectivity to CO_2. SR is favoured at high temperature and, consequently, the CH_4 selectivity in the product stream is lower (Figure S3), reaching a zero value for all fuels except propane (Figure S3c) for $n = 1$. In these conditions, for n much lower than the stoichiometric fuel ratio ($n_{stoic} = 6$), complete methane conversion cannot be achieved.

Parity plots of equilibrium vs experimental conversion are shown in Fig. 6. The experimental data from the literature are reported in Table S2 [[20,61,64,73–118]. As previously stated, all fuels demonstrate a unitary equilibrium conversion, except for methane and biogas. The majority of the analysed catalysts achieve a conversion close to the equilibrium, as indicated by the overlap on the bisector in Fig. 6. Notably, the superposition of experimental and equilibrium values occurs in presence of Ni/Al_2O_3, modified or promoted, and Rh, Ru, Pt supported by Al_2O_3 for methane [73,78–81], for biogas [82,87], propane [58,61] and ethanol [98,101,102,106,118], Cu/CeO_2 and $Cu/ZnO–Al_2O_3$ for methanol [89,92] and the Ni-based catalysts for glycerol [116].

3.2. Comparison of hydrogen yields for different fuels

A comparison of the different fuels studied is shown in Table 5. Methane, biogas and methanol reach their maximum hydrogen yield at a temperature of about 600 °C, while propane, ethanol and glycerol at 700 °C. It suggests that higher temperatures are required for fuels with a higher number of C atoms. Under the maximum yield conditions, methanol achieves a hydrogen yield of 96.10 %, followed by biogas and methane with a yield of about 95.00 %, and then ethanol, glycerol, and propane with 89.66 %, 86.55 % and 84.03 %, respectively.

Taking into account the different number of carbon atoms in the fuels studied, Fig. 7 shows the hydrogen yield at a water-to-C ratio of 3, *i.e.* at the industrial operating conditions of the SRM. According to Section 2.2, the normalised feed ratio is 3 for methane, biogas, and methanol, 9 for propane and glycerol, and 6 for ethanol. Table S3 presents the hydrogen yield at varying pressure and temperature within the investigated ranges for a fixed water-to-C ratio.

As shown in Fig. 7, all fuels reach their maximum hydrogen yield at a pressure of 1 bar (solid line) at a temperature of 700 °C, which is about 86 % for methanol, 85 % for glycerol, 84 % for methane, biogas and ethanol, and 83 % for propane. In these conditions, the ranking of the fuels formulated in terms of hydrogen yields is as follows:

Methanol > Glycerol > Biogas ~ Ethanol > Methane > Propane (@ 700 °C and 1 bar)

At maximum temperature analysed (1000 °C), the ranking is completely different. Glycerol (blue solid curve) is the fuel most affected by the increase in temperature, in fact it shows the greatest decrease in yield. In these conditions, the ranking of the fuels formulated in terms of hydrogen yields is as follows:

Methane > Methanol > Biogas ~ Ethanol ~ Propane > Glycerol (@ 1000 °C and 1 bar)

With increasing pressure, the maximum hydrogen yield is reached at a temperature of 1000 °C for both 20 and 40 bar, except for glycerol, which reaches its maximum yield at 900 °C for 20 bar. At 20 bar (dashed line), almost all fuels achieve a hydrogen yield in the range of 76–80 %, according to the hierarchy given below:

Methane > Methanol > Biogas ~ Ethanol > Glycerol ~ Propane (@ 20 bar and 1000 °C)

At a pressure of 40 bar (dotted line), the yield achieved in the following order is in the range of 75–78 %, which is lower than at lower pressures, being thermodynamically unfavourable conditions. In this conditions, the ranking of the fuels formulated in terms of hydrogen yields is as follows:

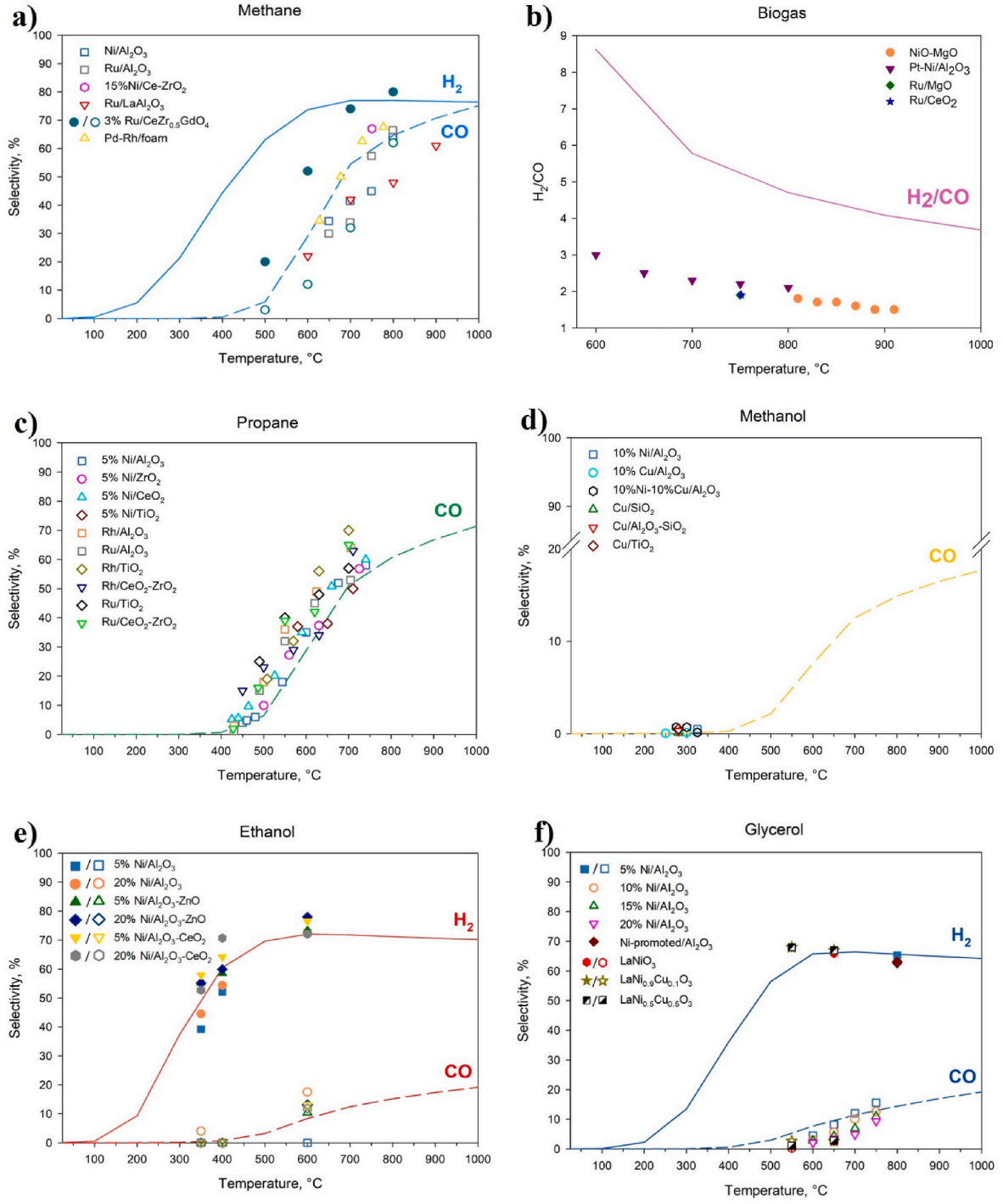

Fig. 9. Comparison between equilibrium results (lines) and experimental data (symbols) for the selectivity to hydrogen and CO as temperature function (water-to-C = 3, P = 1 bar) for steam reforming of: a) methane, b) biogas, c) propane, d) methanol, e) ethanol and f) glycerol.

Methanol > Methane ~ Biogas ~ Ethanol > Glycerol > Propane (@ 40 bar and 1000 °C)

As the pressure increases, its effect pressure is less marked.

The maximum hydrogen yields obtained under the temperature and pressure conditions studied, setting the water-to-C ratio at 3, are shown in Fig. 8. In particular, the bubble sizes are parametric in the yield as to observe the fuel hierarchy for given operating conditions.

Fig. 9 illustrates the selectivity to hydrogen and/or to carbon monoxide when the water-to-C ratio is fixed at 3, as compared to experimental data in the presence of various catalysts proposed in the literature (Table S4) [61,77,84,113,118–129]. In particular, for each fuel the selectivity is plotted against temperature at fixed pressure of 1 bar and with water-to-fuel ratio n of 3 for methane (Fig. 9a), 3 for biogas (Fig. 9b), for propane (Fig. 9c), 3 for methanol (Fig. 9d), 6 for ethanol (Fig. 9e), and 9 for glycerol (Fig. 9f). The provided experimental data from literature can be found in Table S4 of the Supplementary Materials including catalyst, operating conditions, temperature, and selectivity. In Fig. 9, filled symbols correspond to selectivity to H_2, while blanks represent selectivity to CO. Furthermore, due to the limited availability of S_{H_2} and S_{CO} data, the H_2/CO molar ratio for biogas was provided. Notably, for methane and propane (Fig. 9a,c), the definition of selectivity is as follows [61]:

Table 6
Heat duty required at reactor, Q_R, and at heat exchanger, Q_{HE} (and their sum Q), CO_2 mass flow produced during reactions, $m_{CO_2,R}$, and CO_2 emitted with the flue gases, $m_{CO_2\,flue\ gases}$ (and their sum m_{CO_2}), at process operating conditions at which the maximum hydrogen yield is achieved for fixed water-to-C ratio (P = 1 bar, water-to-C = 3, T_R = 700 °C).

Fuel	n	T_{IN}, °C	Q_R, Kcal/h	Q_{HE}, Kcal/h	Q, Kcal/h	$m_{CO_2,R}$, Kg/h	$m_{CO_2\,flue\ gases}$, Kg/h	m_{CO_2}, Kg/h	n_{H_2}, Kmol/h
Methane	3	250	67411.99	40652.86	108064.85	18.77	28.14	46.91	3.34
Biogas	3	250	56093.24	40657.90	96751.14	24.18	23.41	47.59	2.55
Propane	9	250	166283.80	120414.91	286698.71	62.07	69.41	131.48	8.24
Methanol	3	120	45222.51	45849.42	91071.93	26.39	18.88	45.27	2.58
Ethanol	6	150	99800.17	85753.88	185554.04	48.69	41.66	90.34	5.05
Glycerol	9	300	99133.19	147183.76	246316.95	86.74	41.38	128.11	5.94

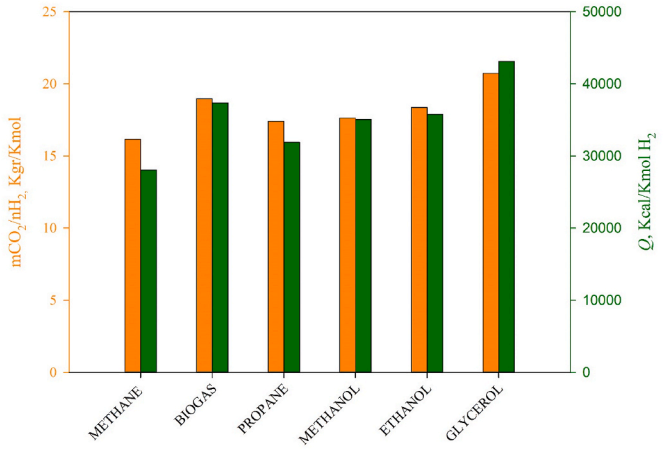

Fig. 10. Global duty demand, Q, and mCO_2/nH_2 for at maximum hydrogen yield operating conditions (700 °C, 1 bar) for water-to-C ratio equals to 3.

$$S_{CO} = \frac{F_{CO}}{F_{CO} + F_{CO_2} + F_{CH_4}} \bullet 100 \tag{3.1}$$

As can be seen from Fig. 9, the thermodynamic study leads to results which are achieved by most of the catalysts analysed. This overlap validates the thermodynamic study as a good starting point for the design of reactor configurations, development of catalysts, economic analysis, etc. Nobel metal-based catalysts, such as Ru/Al_2O_3 and Pd–Rh/ foam [121], lead to about equilibrium CO selectivity for methane steam reforming (Fig. 9a), while only few data are available in literature for biogas in the feed ratio analysed $CH_4/CO_2/H_2O$ = 1/0.33/3, so different feed ratios are shown in Fig. 9b as an example [84,122,123]. In the case of propane (Fig. 9c), all catalysts (Ni- or Nobel metal-based, supported by Al_2O_3, CeO_2, TiO_2 or mixtures) developed by Ramantani et al. [61] and Kokka et al. [124] achieve the maximum CO selectivity. The temperature range investigated in the literature for steam reforming methanol is around 200–300 °C. In this range, the CO selectivity is less than 2 % in good agreement with thermodynamics for different catalysts (Fig. 9d) [126,127]. The selectivity to hydrogen and to CO are close to that predicted by thermodynamics for ethanol steam reforming in the presence of Ni-based catalysts, with overlapping results from Ni/A-l_2O_3-modified [118]. For temperatures above 600 °C, the selectivities calculated by thermodynamics are achieved using the 10 % Ni/Al_2O_3 catalyst in the context of glycerol (Fig. 9d) [113].

3.3. Energy demand and CO_2 emission

Under the operating conditions resulting in maximum hydrogen yield in the analysed case of fixed water-to-C ratio (T_R = 700 °C, P = 1 bar), the following contributions were estimated: (i) the thermal power Q_R required by the reactor; (ii) thermal power required by the heat exchanger to pre-heat the streams to T_{IN}, Q_{HE}; (iii) the CO_2 mass flow rate generated during the reactions $m_{CO_2,R}$, and (iv) the CO_2 emitted with

Table 7
Summary of the normal operating conditions in terms of pressure, water-to-fuel ratio and inlet temperature T_{IN}, heat duty required at reactor, Q_R, and at heat exchanger, Q_{HE}, CO_2 mass flow produced during reactions, $m_{CO_2,R}$, CO_2 emitted with the flue gases, $m_{CO_2\,flue\ gases}$, produced moles of hydrogen n_{H_2} and amount of carbon dioxide globally emitted per mole oh hydrogen produced m_{CO_2}/n_{H_2}.

Fuel	P, bar	n	T_{IN}, °C	T_R, °C	Q_{HE}, Kcal/h	Q_R, Kcal/h	$m_{CO_2,R}$, Kg/h	$m_{CO_2\,flue\ gases}$, Kg/h	n_{H_2}, Kmol/h	m_{CO_2}/n_{H_2}, Kg/Kmol
Methane	20	3	250	600	40069.6	27460.3	10.50	11.46	1.069	20.52
				800		60901.4	14.66	24.42	2.53	15.83
				1000		85457.2	10.92	35.66	3.19	14.57
				1200		97451.3	8.29	40.67	3.18	15.37
Biogas	7	2.5	250	600	34101.4	42277.1	24.85	17.64	2.14	19.85
				800		60120.0	18.20	25.04	2.43	17.76
				1000		69949.7	13.44	29.195	2.33	18.27
				1200		79641.6	10.54	33.24	2.26	19.30
Propane	20	3	250	600	42743.51	26085.29	27.94	10.89	0.98	39.56
				800		82977.27	18.42	34.63	3.05	17.39
				1000		150825.84	4.80	62.95	5.53	12.25
				1200		187208.02	1.02	78.14	6.56	12.07
Methanol	1	3	120	300	45849.4	<0	13.18	–	0.199	–
				400		1779.01	18.47	11.46	0.701	42.67
				500		17343.11	26.23	31.91	1.58	36.72
				600		35368.21	29.46	35.66	2.42	26.85
Ethanol	1	3	150	400	49350.0	2148.68	29.62	0.897	0.738	41.34
				600		54260.66	37.60	22.65	3.29	18.29
				800		97474.31	23.22	40.68	4.50	14.19
				900		105302.95	19.25	43.95	4.43	14.25
Glycerol	1	7	300	500	120712.1	22378.4	84.83	9.34	3.33	28.22
				700		92909.6	78.54	38.78	5.73	20.46
				900		122740.6	60.06	51.23	5.36	20.74
				1000		137020.4	53.35	57.19	5.21	21.20

the flue gases produced by an auxiliary stream of methane and stoichiometric air supplied to the burner, $m_{CO_2,flue\ gases}$. Results are reported in Table 6.

Propane has the highest total heat demand and leads to the largest total amount of CO_2 produce, while methanol has the lowest. However, propane also leads to the highest hydrogen production under these conditions. Normalising these results to the amount of hydrogen produced under these conditions (Fig. 10) shows that the largest CO_2 emissions per unit of hydrogen are due to biogas and glycerol. A successful trade-off between hydrogen produced, heat required, and CO_2 emissions is given by methane and methanol.

The maximum hydrogen yield operating conditions ($P = 1$ bar, *water-to-C = 3,* $T_R = 700$ °C) operationally do not correspond to the industrial operating conditions of the process, reported instead in Table 4. Therefore, Table 7 shows the heat and CO_2 emissions under the operating conditions of the steam reforming process under typical industrial conditions. The heat required for the heat exchanger, Q_{HE}, is highly dependent on the inlet temperature, T_{IN}, and the total flow rate fed. Indeed, Q_{HE} in the case of glycerol is an order of magnitude higher than the other fuels because $T_{IN} = 300$ °C must be reached in order to have glycerol into the gas phase and the total flow rate (8 kmol/h) is higher than the other fuels. In the case of methanol, at 300 °C, from a thermodynamic point of view the WGS reaction (exothermic) is favoured, so the total heat is negative. This implies that the catalyst should be highly selective so that the desired reaction (SR) could takes place [42]. As the temperature and heat required to sustain the reaction increase, the CO_2 emissions associated with the combustion of the auxiliary current in the burners increase. Both under normal operating conditions and under the conditions of maximum hydrogen yield (Table 5), glycerol leads to the highest carbon dioxide emissions, both in the reactor output and in the exhaust gases, which are, however, comparable to those of other fuels when normalised with respect to produced hydrogen. CO_2 emissions per unit hydrogen show a non-monotonic trend (Table 7) with increasing temperature; after reaching the minimum value, the increase is related to rWGS.

4. Conclusions

Today, hydrogen is mainly produced by steam reforming (SR) methane, but attempts are being made to integrate environmentally friendly fuels such as bio-alcohols, biogas, and LPG into the traditional steam reforming process. In this scenario, we propose a thermodynamic study of the steam reforming process of different fuels. The analysis was carried out using Gibbs free energy minimisation method, investigating the effect of operating conditions (temperature, pressure and water-to-fuel ratio) on the performance of SR, and the energy demand and CO_2 emissions under typical operating conditions.

Fuel conversion is always complete, but the yield of hydrogen varies depending on operative conditions. The hydrogen yield decreases with pressure, while it shows a non-monotonic trend with temperature, due to the consumption of hydrogen by the rWGS reaction. At a fixed water-to-carbon ratio of 3, atmospheric pressure, and 700 °C, the fuels reach their maximum yields between 83 % and 86 %, with methanol showing the highest value. Increasing pressure leads to higher yields at higher temperature, with methane reaching its maximum at 20 bar and methanol at 40 bar, both at 1000 °C. The analysis also considered heat duty and CO_2 emissions. Biogas and methanol have the highest heat demand and CO_2 emissions per mole of hydrogen produced, while propane and glycerol have the lowest values, respectively.

Overall, the thermodynamic analysis allows a better understanding of different fuels performances in terms of hydrogen yield, energy demand, and CO_2 emissions. This result can drive future research and decision-making in fuel conversion processes, enabling the identification of fuels with higher efficiency and lower environmental impact and represent a useful benchmark for experimental and industrial results.

Funding

This research did not receive any specific grant from funding agencies in the public, commercial, or not-for-profit sectors.

Declaration of competing interest

The authors declare that they have no known competing financial interests or personal relationships that could have appeared to influence the work reported in this paper.

Appendix A. Supplementary data

Supplementary data to this article can be found online at https://doi.org/10.1016/j.ijhydene.2023.11.215.

References

[1] Lutz AE, Bradshaw RW, Keller JO, Witmer DE. Thermodynamic analysis of hydrogen production by steam reforming, vol. 28; 2003.
[2] Abe JO, Popoola API, Ajenifuja E, Popoola OM. Hydrogen energy, economy and storage: review and recommendation. Int J Hydrogen Energy 2019;44:15072–86. https://doi.org/10.1016/J.IJHYDENE.2019.04.068.
[3] Tashie-Lewis BC, Nnabuife SG. Hydrogen production, distribution, storage and power conversion in a hydrogen economy - a technology review. Chemical Engineering Journal Advances 2021;8. https://doi.org/10.1016/j.ceja.2021.100172.
[4] Yue M, Lambert H, Pahon E, Roche R, Jemei S, Hissel D. Hydrogen energy systems: a critical review of technologies, applications, trends and challenges. Renew Sustain Energy Rev 2021;146. https://doi.org/10.1016/j.rser.2021.111180.
[5] Halder P, Babaie M, Salek F, Haque N, Savage R, Stevanovic S, et al. Advancements in hydrogen production, storage, distribution and refuelling for a sustainable transport sector: hydrogen fuel cell vehicles. Int J Hydrogen Energy 2023. https://doi.org/10.1016/J.IJHYDENE.2023.07.204.
[6] Muthukumar P, Kumar A, Afzal M, Bhogilla S, Sharma P, Parida A, et al. Review on large-scale hydrogen storage systems for better sustainability. Int J Hydrogen Energy 2023;48:33223–59. https://doi.org/10.1016/J.IJHYDENE.2023.04.304.
[7] IEA. The future of hydrogen. Seizing today's opportunities; 2019.
[8] Boretti A, Banik BK. Advances in hydrogen production from natural gas reforming. Advanced Energy and Sustainability Research 2021;2:2100097. https://doi.org/10.1002/aesr.202100097.
[9] Collodi G. Hydrogen production via steam reforming with CO2 capture. Chem Eng Trans 2010;19:37–42. https://doi.org/10.3303/CET1019007.
[10] Bepari S, Kuila D. Steam reforming of methanol, ethanol and glycerol over nickel-based catalysts-A review. Int J Hydrogen Energy 2020;45:18090–113. https://doi.org/10.1016/j.ijhydene.2019.08.003.
[11] Buffoni I, Santori G, Pompeo F, Nichio N. Steam reforming of alcohols for hydrogen production, vol. 3; 2014.
[12] Pal DB, Singh A, Bhatnagar A. A review on biomass based hydrogen production technologies. Int J Hydrogen Energy 2022;47:1461–80. https://doi.org/10.1016/J.IJHYDENE.2021.10.124.
[13] Ranjekar AM, Yadav GD. Steam reforming of methanol for hydrogen production: a critical analysis of Catalysis, processes, and scope. Ind Eng Chem Res 2021;60:89–113. https://doi.org/10.1021/acs.iecr.0c05041.
[14] Melikoglu M, Singh V, Leu SY, Webb C, Lin CSK. Biochemical production of bioalcohols. Handbook of biofuels production: processes and technologies. second ed. Elsevier Inc.; 2016. p. 237–58. https://doi.org/10.1016/B978-0-08-100455-5.00009-6.
[15] Abdul Raman AA, Tan HW, Buthiyappan A. Two-step purification of glycerol as a value added by product from the biodiesel production process. Front Chem 2019;7. https://doi.org/10.3389/fchem.2019.00774.
[16] Qureshi F, Yusuf M, Pasha AA, Khan HW, Imteyaz B, Irshad K. Sustainable and energy efficient hydrogen production via glycerol reforming techniques: a review. Int J Hydrogen Energy 2022;47:41397–420. https://doi.org/10.1016/j.ijhydene.2022.04.010.
[17] Adeniyi AG, Ighalo JO. A review of steam reforming of glycerol. Chemical Papers 2019;73:2619–35. https://doi.org/10.1007/s11696-019-00840-8.
[18] Rakib MA, Grace JR, Lim CJ, Elnashaie SSEH, Ghiasi B. Steam reforming of propane in a fluidized bed membrane reactor for hydrogen production. Renew Energy 2010;35:6276–90. https://doi.org/10.1016/j.ijhydene.2010.03.136.
[19] Cui X, Kær SK. Thermodynamic analysis of steam reforming and oxidative steam reforming of propane and butane for hydrogen production. Int J Hydrogen Energy 2018;43:13009–21. https://doi.org/10.1016/J.IJHYDENE.2018.05.083.
[20] Kokka A, Katsoni A, Yentekakis IV, Panagiotopoulou P. Hydrogen production via steam reforming of propane over supported metal catalysts. Int J Hydrogen Energy 2020;45:14849–66. https://doi.org/10.1016/j.ijhydene.2020.03.194.
[21] Zhao X, Joseph B, Kuhn J, Ozcan S. Biogas reforming to syngas: a review. iScience 2020;23:101082. https://doi.org/10.1016/j.isci.
[22] Minh DP, Siang TJ, Vo DVN, Phan TS, Ridart C, Nzihou A, et al. Hydrogen production from biogas reforming: an overview of steam reforming, dry

reforming, dual reforming, and tri-reforming of methane. In: Hydrogen supply chain: design, deployment and operation. Elsevier; 2018. p. 111–66. https://doi.org/10.1016/B978-0-12-811197-0.00004-X.
[23] Ji M, Wang J. Review and comparison of various hydrogen production methods based on costs and life cycle impact assessment indicators. Int J Hydrogen Energy 2021;46:38612–35. https://doi.org/10.1016/J.IJHYDENE.2021.09.142.
[24] Levalley TL, Richard AR, Fan M. The progress in water gas shift and steam reforming hydrogen production technologies - a review. Int J Hydrogen Energy 2014;39:16983–7000. https://doi.org/10.1016/j.ijhydene.2014.08.041.
[25] Su B, Lin F, Ma J, Huang S, Wang Y, Zhang X, et al. System integration of multi-grade exploitation of biogas chemical energy driven by solar energy. Energy 2022;241. https://doi.org/10.1016/j.energy.2021.122857.
[26] Chen L, Qi Z, Zhang S, Su J, Somorjai GA. Catalytic hydrogen production from methane: a review on recent progress and prospect. Catalysts 2020;10. https://doi.org/10.3390/catal10080858.
[27] Barelli L, Bidini G, Gallorini F, Servili S. Hydrogen production through sorption-enhanced steam methane reforming and membrane technology: a review. Energy 2008;33:554–70. https://doi.org/10.1016/j.energy.2007.10.018.
[28] Summa P, Samojeden B, Motak M. Dry and steam reforming of methane. Comparison and analysis of recently investigated catalytic materials. A short review. Polish Journal of Chemical Technology 2019;21:31–7. https://doi.org/10.2478/pjct-2019-0017.
[29] Zhang H, Sun Z, Hu YH. Steam reforming of methane: current states of catalyst design and process upgrading. Renew Sustain Energy Rev 2021;149. https://doi.org/10.1016/j.rser.2021.111330.
[30] Singh S, Jain S, Ps V, Tiwari AK, Nouni MR, Pandey JK, et al. Hydrogen: a sustainable fuel for future of the transport sector. Renew Sustain Energy Rev 2015;51:623–33. https://doi.org/10.1016/j.rser.2015.06.040.
[31] Hussien AGS, Polychronopoulou K. A review on the different aspects and challenges of the dry reforming of methane (DRM) reaction. Nanomaterials 2022;12. https://doi.org/10.3390/nano12193400.
[32] Angeli SD, Turchetti L, Monteleone G, Lemonidou AA. Catalyst development for steam reforming of methane and model biogas at low temperature. Appl Catal, B 2016;181:34–46. https://doi.org/10.1016/j.apcatb.2015.07.039.
[33] Masoudi Soltani S, Lahiri A, Bahzad H, Clough P, Gorbounov M, Yan Y. Sorption-enhanced steam methane reforming for combined CO2 capture and hydrogen production: a state-of-the-art review. Carbon Capture Science & Technology 2021;1:100003. https://doi.org/10.1016/j.ccst.2021.100003.
[34] Li D, Xu R, Gu Z, Zhu X, Qing S, Li K. Chemical-looping conversion of methane: a review. Energy Technol 2020;8. https://doi.org/10.1002/ente.201900925.
[35] Cho Y, Yamaguchi A, Miyauchi M. Photocatalytic methane reforming: recent advances. Catalysts 2021;11:1–41. https://doi.org/10.3390/catal11010018.
[36] Han B, Wei W, Li M, Sun K, Hu YH. A thermo-photo hybrid process for steam reforming of methane: highly efficient visible light photocatalysis. Chem Commun 2019;55:7816–9. https://doi.org/10.1039/c9cc04193a.
[37] Feng J, Sun X, Li Z, Hao X, Fan M, Ning P, et al. Plasma-assisted reforming of methane. Adv Sci 2022;9. https://doi.org/10.1002/advs.202203221.
[38] Collins-Martinez V, Escobedo Bretado M, Meléndez Zaragoza M, Salinas Gutiérrez J, Ortiz AL. Absorption enhanced reforming of light alcohols (methanol and ethanol) for the production of hydrogen: thermodynamic modeling. Int J Hydrogen Energy 2013;38:12539–53. https://doi.org/10.1016/j.ijhydene.2012.11.146.
[39] Nikazar S. Hydrogen production from methanol steam reforming in a microwave reactor a thesis submitted to the graduate school of natural and applied sciences of MIDDLE EAST. TECHNICAL UNIVERSITY; 2019.
[40] Kang J, Song Y, Kim T, Kim S. Recent trends in the development of reactor systems for hydrogen production via methanol steam reforming. Int J Hydrogen Energy 2022;47:3587–610. https://doi.org/10.1016/j.ijhydene.2021.11.041.
[41] Kappis K, Papavasiliou J, Avgouropoulos G. Methanol reforming processes for fuel cell applications. Energies 2021;14. https://doi.org/10.3390/en14248442.
[42] Sá S, Silva H, Brandão L, Sousa JM, Mendes A. Catalysts for methanol steam reforming—a review. Appl Catal, B 2010;99:43–57. https://doi.org/10.1016/J.APCATB.2010.06.015.
[43] Anil S, Indraja S, Singh R, Appari S, Roy B. A review on ethanol steam reforming for hydrogen production over Ni/Al2O3 and Ni/CeO2 based catalyst powders. Int J Hydrogen Energy 2022;47:8177–213. https://doi.org/10.1016/j.ijhydene.2021.12.183.
[44] Ogo S, Sekine Y. Recent progress in ethanol steam reforming using non-noble transition metal catalysts: a review. Fuel Process Technol 2020;199. https://doi.org/10.1016/j.fuproc.2019.106238.
[45] Khaodee W, Jiwanuruk T, Ountaksinkul K, Charojrochkul S, Charoensuk J, Wongsakulphasatch S, et al. Compact heat integrated reactor system of steam reformer, shift reactor and combustor for hydrogen production from ethanol. Processes 2020;8. https://doi.org/10.3390/PR8060708.
[46] Bagnato G, Iulianelli A, Sanna A, Basile A. Glycerol production and transformation: a critical review with particular emphasis on glycerol reforming reaction for producing hydrogen in conventional and membrane reactors. Membranes 2017;7. https://doi.org/10.3390/membranes7020017.
[47] Schwengber CA, Alves HJ, Schaffner RA, Da Silva FA, Sequinel R, Bach VR, et al. Overview of glycerol reforming for hydrogen production. Renew Sustain Energy Rev 2016;58:259–66. https://doi.org/10.1016/j.rser.2015.12.279.
[48] Fasolini A, Cespi D, Tabanelli T, Cucciniello R, Cavani F. Hydrogen from renewables: a case study of glycerol reforming. Catalysts 2019;9. https://doi.org/10.3390/catal9090722.
[49] Ismaila A, Chen X, Gao X, Fan X. Thermodynamic analysis of steam reforming of glycerol for hydrogen production at atmospheric pressure. Front Chem Sci Eng 2021;15:60–71. https://doi.org/10.1007/s11705-020-1975-0.
[50] Roslan NA, Abidin SZ, Ideris A, Vo DVN. A review on glycerol reforming processes over Ni-based catalyst for hydrogen and syngas productions. Int J Hydrogen Energy 2020;45:18466–89. https://doi.org/10.1016/j.ijhydene.2019.08.211.
[51] Wang C, Chen Y, Cheng Z, Luo X, Jia L, Song M, et al. Sorption-Enhanced Steam Reforming of Glycerol for Hydrogen Production over a NiO/NiAl 2 O 4 Catalyst and Li 2 ZrO 3-Based Sorbent 2015. https://doi.org/10.1021/acs.energyfuels.5b01941.
[52] Sánchez N, Encinar JM, González JF. Sorption enhanced steam reforming of glycerol: use of La-modified Ni/Al2O3 as catalyst. Ind Eng Chem Res 2016;55:3736–41. https://doi.org/10.1021/acs.iecr.5b04084.
[53] Li H, Zhang Y, Fu P, Wei R, Li Z, Dai L, et al. Chemical looping steam reforming of glycerol for hydrogen production over NiO-Fe 2 O 3 /Al 2 O 3 oxygen carriers 2022. https://doi.org/10.1039/d2ra04303c.
[54] Manfro RL, Da Costa AF, Ribeiro NFP, Souza MMVM. Hydrogen production by aqueous-phase reforming of glycerol over nickel catalysts supported on CeO2. Fuel Process Technol 2011;92:330–5. https://doi.org/10.1016/j.fuproc.2010.09.024.
[55] Patcharavorachot Y, Chery-Rod N, Nudchapong S, Authayanun S, Arpornwichanop A. Hydrogen production form glycerol steam reforming in supercritical water with CO2 absorption unit. Chem Eng Trans 2014;39:349–54. https://doi.org/10.3303/CET1439059.
[56] Seadira TWP, Baloyi SJ, Masuku CM, Scurrell MS. Solar photocatalytic hydrogen production from glycerol reforming using ternary Cu/THS/Graphene. In: IOP conf ser mater Sci Eng, vol. 655. Institute of Physics Publishing; 2019. https://doi.org/10.1088/1757-899X/655/1/012049.
[57] Ramantani T, Bampos G, Vavatsikos A, Vatskalis G, Kondarides DI. Propane steam reforming over catalysts derived from noble metal (Ru, Rh)-substituted LaNiO3 and La0.8Sr0.2NiO3 perovskite precursors. Nanomaterials 2021;11. https://doi.org/10.3390/nano11081931.
[58] Kokka A, Ramantani T, Panagiotopoulou P. Effect of operating conditions on the performance of Rh/TiO2 catalyst for the reaction of LPG steam reforming. Catalysts 2021;11:1–21. https://doi.org/10.3390/catal11030374.
[59] Zhang L, Wang X, Tan B, Ozkan US. Effect of preparation method on structural characteristics and propane steam reforming performance of Ni-Al2O3 catalysts. J Mol Catal Chem 2009;297:26–34. https://doi.org/10.1016/j.molcata.2008.09.011.
[60] Borges RP, Moura LG, Spivey JJ, Noronha FB, Hori CE. Hydrogen production by steam reforming of LPG using supported perovskite type precursors. Int J Hydrogen Energy 2020;45:21166–77. https://doi.org/10.1016/J.IJHYDENE.2020.05.183.
[61] Ramantani T, Evangeliou V, Kormentzas G, Kondarides DI. Hydrogen production by steam reforming of propane and LPG over supported metal catalysts. Appl Catal, B 2022;306. https://doi.org/10.1016/j.apcatb.2022.121129.
[62] De Vasconcelos BR, Lavoie JM. Is dry reforming the solution to reduce natural gas carbon footprint? International Journal of Energy Production and Management 2018;3:44–56. https://doi.org/10.2495/EQ-V3-N1-44-56.
[63] Parente M, Soria MA, Madeira LM. Hydrogen and/or syngas production through combined dry and steam reforming of biogas in a membrane reactor: a thermodynamic study. Renew Energy 2020;157:1254–64. https://doi.org/10.1016/j.renene.2020.05.023.
[64] Saeidabad NG, Noh YS, Eslami AA, Song HT, Kim HD, Fazeli A, et al. A review on catalysts development for steam reforming of biodiesel derived glycerol; promoters and supports. Catalysts 2020;10:1–22. https://doi.org/10.3390/catal10080910.
[65] Perry RH, Green DW, Maloney JO. Perry's chemical Engineers' hand-book. 1999. New York.
[66] Wang X, Wang N, Wang L. Hydrogen production by sorption enhanced steam reforming of propane: a thermodynamic investigation. Int J Hydrogen Energy 2011;36:466–72. https://doi.org/10.1016/j.ijhydene.2010.09.021.
[67] Faungnawakij K, Kikuchi R, Eguchi K. Thermodynamic evaluation of methanol steam reforming for hydrogen production. J Power Sources 2006;161:87–94. https://doi.org/10.1016/j.jpowsour.2006.04.091.
[68] Pashchenko D. Thermodynamic equilibrium analysis of combined dry and steam reforming of propane for thermochemical waste-heat recuperation. Int J Hydrogen Energy 2017;42:14926–35. https://doi.org/10.1016/j.ijhydene.2017.04.284.
[69] Xing S, Zhao C, Ban S, Liu Y, Wang H. Thermodynamic performance analysis of the influence of multi-factor coupling on the methanol steam reforming reaction. Int J Hydrogen Energy 2020;45:7015–24. https://doi.org/10.1016/j.ijhydene.2019.12.192.
[70] Techonology Aspen. Aspen Physical Property System - Physical Property Methods and Models 2001;11(1).
[71] Lima Da Silva A, Müller IL. Hydrogen production by sorption enhanced steam reforming of oxygenated hydrocarbons (ethanol, glycerol, n-butanol and methanol): thermodynamic modelling. Int J Hydrogen Energy 2011;36:2057–75. https://doi.org/10.1016/j.ijhydene.2010.11.051.
[72] Adhikari S, Fernando S, Gwaltney SR, Filip To SD, Mark Bricka R, Steele PH, et al. A thermodynamic analysis of hydrogen production by steam reforming of glycerol. Int J Hydrogen Energy 2007;32:2875–80. https://doi.org/10.1016/j.ijhydene.2007.03.023.
[73] Kim H-W, Kang K-M, Kwak H-Y, Kim JH. Preparation of supported Ni catalysts on various metal oxides with core/shell structures and their tests for the steam

reforming of methane. Chem Eng J 2011;168:775–83. https://doi.org/10.1016/j.cej.2010.11.045.
[74] You X, Wang X, Ma Y, Liu J, Liu W, Xu X, et al. Ni–Co/Al2O3 bimetallic catalysts for CH4 steam reforming: elucidating the role of Co for improving coke resistance. ChemCatChem 2014;6:3377–86. https://doi.org/10.1002/cctc.201402695.
[75] Gonçalves JF, Souza MMVM. Effect of doping niobia over Ni/Al2O3 catalysts for methane steam reforming. Catal Lett 2018;148:1478–89. https://doi.org/10.1007/s10562-018-2359-7.
[76] Miura S, Umemura Y, Shiratori Y, Kitaoka T. In situ synthesis of Ni/MgO catalysts on inorganic paper-like matrix for methane steam reforming. Chem Eng J 2013;229:515–21. https://doi.org/10.1016/j.cej.2013.06.052.
[77] Dong WS, Roh HS, Jun KW, Park SE, Oh YS. Methane reforming over Ni/Ce-ZrO2 catalysts: effect of nickel content. Appl Catal Gen 2002;226:63–72. https://doi.org/10.1016/S0926-860X(01)00883-3.
[78] Oh Y-S, Roh H-S, Jun K-W, Baek Y-S. A highly active catalyst, Ni/Ce–ZrO2/θ-Al2O3, for on-site H2 generation by steam methane reforming: pretreatment effect. Int J Hydrogen Energy 2003;28:1387–92. https://doi.org/10.1016/S0360-3199(03)00029-6.
[79] Ali S, Al-Marri MJ, Abdelmoneim AG, Kumar A, Khader MM. Catalytic evaluation of nickel nanoparticles in methane steam reforming. Int J Hydrogen Energy 2016;41:22876–85. https://doi.org/10.1016/j.ijhydene.2016.08.200.
[80] Dębek R, Motak M, Galvez ME, Da Costa P, Grzybek T. Catalytic activity of hydrotalcite-derived catalysts in the dry reforming of methane: on the effect of Ce promotion and feed gas composition. React Kinet Mech Catal 2017;121:185–208. https://doi.org/10.1007/s11144-017-1167-1.
[81] Vita A, Cristiano G, Italiano C, Pino L, Specchia S. Syngas production by methane oxy-steam reforming on Me/CeO2 (Me = Rh, Pt, Ni) catalyst lined on cordierite monoliths. Appl Catal, B 2015;162:551–63. https://doi.org/10.1016/j.apcatb.2014.07.028.
[82] Park D, Lee C, Moon DJ, Kim T. Design, analysis, and performance evaluation of steam-CO 2 reforming reactor for syngas production in GTL process. Int J Hydrogen Energy 2015;40:11785–90. https://doi.org/10.1016/j.ijhydene.2015.05.030.
[83] Olah GA, Goeppert A, Czaun M, Prakash GKS. Bi-Reforming of methane from any source with steam and carbon dioxide exclusively to metgas (CO–2H 2) for methanol and hydrocarbon synthesis. J Am Chem Soc 2013;135:648–50. https://doi.org/10.1021/ja311796n.
[84] Olah GA, Goeppert A, Czaun M, Mathew T, May RB, Prakash GKS. Single step Bi-reforming and oxidative Bi-reforming of methane (natural gas) with steam and carbon dioxide to metgas (CO-2H $_2$) for methanol synthesis: self-sufficient effective and exclusive oxygenation of methane to methanol with oxygen. J Am Chem Soc 2015;137:8720–9. https://doi.org/10.1021/jacs.5b02029.
[85] Li W, Zhao Z, Ding F, Guo X, Wang G. Syngas production via steam–CO $_2$ dual reforming of methane over LA-Ni/ZrO $_2$ catalyst prepared by <scp>l</scp> -arginine ligand-assisted strategy: enhanced activity and stability. ACS Sustain Chem Eng 2015;3:3461–76. https://doi.org/10.1021/acssuschemeng.5b01277.
[86] Rahmat N, Yaakob Z, Rahman NA, Jahaya SS. Renewable hydrogen-rich syngas from CO2 reforming of CH4 with steam over Ni/MgAl2O4 and its process optimization. Int J Environ Sci Technol 2020;17:843–56. https://doi.org/10.1007/s13762-019-02520-2.
[87] Li M, van Veen AC. Coupled reforming of methane to syngas (2H2-CO) over Mg-Al oxide supported Ni catalyst. Appl Catal Gen 2018;550:176–83. https://doi.org/10.1016/j.apcata.2017.11.004.
[88] Shishido T, Yamamoto Y, Morioka H, Takehira K. Production of hydrogen from methanol over Cu/ZnO and Cu/ZnO/Al2O3 catalysts prepared by homogeneous precipitation: steam reforming and oxidative steam reforming. J Mol Catal Chem 2007;268:185–94. https://doi.org/10.1016/j.molcata.2006.12.018.
[89] Yang S, Zhou F, Liu Y, Zhang L, Chen Y, Wang H, et al. Morphology effect of ceria on the performance of CuO/CeO2 catalysts for hydrogen production by methanol steam reforming. Int J Hydrogen Energy 2019;44:7252–61. https://doi.org/10.1016/j.ijhydene.2019.01.254.
[90] Mateos-Pedrero C, Azenha C, Pt DA, Sousa JM, Mendes A. The influence of the support composition on the physicochemical and catalytic properties of Cu catalysts supported on Zirconia-Alumina for methanol steam reforming. Appl Catal, B 2020;277:119243. https://doi.org/10.1016/j.apcatb.2020.119243.
[91] Patel S, Pant KK. Activity and stability enhancement of copper–alumina catalysts using cerium and zinc promoters for the selective production of hydrogen via steam reforming of methanol. J Power Sources 2006;159:139–43. https://doi.org/10.1016/j.jpowsour.2006.04.008.
[92] Shen J. Influence of preparation method on performance of Cu/Zn-based catalysts for low-temperature steam reforming and oxidative steam reforming of methanol for H2 production for fuel cells. Catal Today 2002;77:89–98. https://doi.org/10.1016/S0920-5861(02)00235-3.
[93] Huang G, Liaw B-J, Jhang C-J, Chen Y-Z. Steam reforming of methanol over CuO/ZnO/CeO2/ZrO2/Al2O3 catalysts. Appl Catal Gen 2009;358:7–12. https://doi.org/10.1016/j.apcata.2009.01.031.
[94] Cai F, Guo Y, Ibrahim JJ, Zhang J, Sun Y. A highly active and stable Pd/MoC catalyst for hydrogen production from methanol decomposition. Appl Catal, B 2021;299:120648. https://doi.org/10.1016/j.apcatb.2021.120648.
[95] Minaei S, Haghighi M, Jodeiri N, Ajamein H, Abdollahifar M. Urea-nitrates combustion preparation of CeO 2 -promoted CuO/ZnO/Al 2 O 3 nanocatalyst for fuel cell grade hydrogen production via methanol steam reforming. Adv Powder Technol 2017;28:842–53. https://doi.org/10.1016/j.apt.2016.12.010.
[96] Iwasa N, Mayanagi T, Ogawa N, Sakata K, Takezawa N. New catalytic functions of Pd–Zn, Pd–Ga, Pd–in, Pt–Zn, Pt–Ga and Pt–in alloys in the conversions of methanol. Catal Lett 1998;54:119–23. https://doi.org/10.1023/A:1019056728333.
[97] Liu Z, Yao S, Johnston-Peck A, Xu W, Rodriguez JA, Senanayake SD. Methanol steam reforming over Ni-CeO2 model and powder catalysts: pathways to high stability and selectivity for H2/CO2 production. Catal Today 2018;311:74–80. https://doi.org/10.1016/j.cattod.2017.08.041.
[98] Han SJ, Bang Y, Song JH, Yoo J, Park S, Kang KH, et al. Hydrogen production by steam reforming of ethanol over dual-templated Ni–Al2O3 catalyst. Catal Today 2016;265:103–10. https://doi.org/10.1016/j.cattod.2015.07.041.
[99] Alberton AL, Souza MMVM, Schmal M. Carbon formation and its influence on ethanol steam reforming over Ni/Al2O3 catalysts. Catal Today 2007;123:257–64. https://doi.org/10.1016/j.cattod.2007.01.062.
[100] Akande AJ, Idem RO, Dalai AK. Synthesis, characterization and performance evaluation of Ni/Al2O3 catalysts for reforming of crude ethanol for hydrogen production. Appl Catal Gen 2005;287:159–75. https://doi.org/10.1016/j.apcata.2005.03.046.
[101] Ramírez-Hernández GY, Viveros-García T, Fuentes-Ramírez R, Galindo-Esquivel IR. Promoting behavior of yttrium over nickel supported on alumina-yttria catalysts in the ethanol steam reforming reaction. Int J Hydrogen Energy 2016;41:9332–43. https://doi.org/10.1016/j.ijhydene.2016.04.080.
[102] Zhao X, Lu G. Modulating and controlling active species dispersion over Ni–Co bimetallic catalysts for enhancement of hydrogen production of ethanol steam reforming. Int J Hydrogen Energy 2016;41:3349–62. https://doi.org/10.1016/j.ijhydene.2015.09.063.
[103] De Rogatis L, Montini T, Lorenzut B, Fornasiero P. NixCuy/Al2O3 based catalysts for hydrogen production. Energy Environ Sci 2008. https://doi.org/10.1039/b805426f.
[104] Barattini L, Ramis G, Resini C, Busca G, Sisani M, Costantino U. Reaction path of ethanol and acetic acid steam reforming over Ni–Zn–Al catalysts. Flow reactor studies. Chem Eng J 2009;153:43–9. https://doi.org/10.1016/j.cej.2009.06.002.
[105] Anjaneyulu C, Costa LOO da, Ribeiro MC, Rabelo-Neto RC, Mattos LV, Venugopal A, et al. Effect of Zn addition on the performance of Ni/Al2O3 catalyst for steam reforming of ethanol. Appl Catal Gen 2016;519:85–98. https://doi.org/10.1016/j.apcata.2016.03.008.
[106] Han SJ, Bang Y, Yoo J, Park S, Kang KH, Choi JH, et al. Hydrogen production by steam reforming of ethanol over P123-assisted mesoporous Ni–Al2O3–ZrO2 xerogel catalysts. Int J Hydrogen Energy 2014;39:10445–53. https://doi.org/10.1016/j.ijhydene.2014.05.014.
[107] Choong CKS, Huang L, Zhong Z, Lin J, Hong L, Chen L. Effect of calcium addition on catalytic ethanol steam reforming of Ni/Al2O3: II. Acidity/basicity, water adsorption and catalytic activity. Appl Catal Gen 2011;407:155–62. https://doi.org/10.1016/j.apcata.2011.08.038.
[108] Greluk M, Gac W, Rotko M, Słowik G, Turczyniak-Surdacka S. Co/CeO2 and Ni/CeO2 catalysts for ethanol steam reforming: effect of the cobalt/nickel dispersion on catalysts properties. J Catal 2021;393:159–78. https://doi.org/10.1016/j.jcat.2020.11.009.
[109] Wang F, Zhang L, Deng J, Zhang J, Han B, Wang Y, et al. Embedded Ni catalysts in Ni-O-Ce solid solution for stable hydrogen production from ethanol steam reforming reaction. Fuel Process Technol 2019;193:94–101. https://doi.org/10.1016/j.fuproc.2019.05.004.
[110] Pinton N, Vidal MV, Signoretto M, Martínez-Arias A, Cortés Corberán V. Ethanol steam reforming on nanostructured catalysts of Ni, Co and CeO 2 : influence of synthesis method on activity, deactivation and regenerability. Catal Today 2017;296:135–43. https://doi.org/10.1016/j.cattod.2017.06.022.
[111] Niazi Z, Irankhah A, Wang Y, Arandiyan H. Cu, Mg and Co effect on nickel-ceria supported catalysts for ethanol steam reforming reaction. Int J Hydrogen Energy 2020;45:21512–22. https://doi.org/10.1016/j.ijhydene.2020.06.001.
[112] Dou B, Wang C, Song Y, Chen H, Xu Y. Activity of Ni–Cu–Al based catalyst for renewable hydrogen production from steam reforming of glycerol. Energy Convers Manag 2014;78:253–9. https://doi.org/10.1016/j.enconman.2013.10.067.
[113] Zarei Senseni A, Meshkani F, Rezaei M. Steam reforming of glycerol on mesoporous nanocrystalline Ni/Al 2 O 3 catalysts for H 2 production. Int J Hydrogen Energy 2016;41:20137. https://doi.org/10.1016/j.ijhydene.2016.08.046. –46.
[114] Parlar Karakoc O, Kibar ME, Akin AN, Yildiz M. Nickel-based catalysts for hydrogen production by steam reforming of glycerol. Int J Environ Sci Technol 2019;16:5117–24. https://doi.org/10.1007/s13762-018-1875-8.
[115] Zarei Senseni A, Rezaei M, Meshkani F. Glycerol steam reforming over noble metal nanocatalysts. Chem Eng Res Des 2017;123:360–6. https://doi.org/10.1016/j.cherd.2017.05.020.
[116] Adhikari S, Fernando SD, Haryanto A. Hydrogen production from glycerin by steam reforming over nickel catalysts. Renew Energy 2008;33:1097–100. https://doi.org/10.1016/j.renene.2007.09.005.
[117] Chen H, Ding Y, Cong NT, Dou B, Dupont V, Ghadiri M, et al. A comparative study on hydrogen production from steam-glycerol reforming: thermodynamics and experimental. Renew Energy 2011;36:779–88. https://doi.org/10.1016/j.renene.2010.07.026.
[118] Shtyka O, Dimitrova Z, Ciesielski R, Kedziora A, Mitukiewicz G, Leyko J, et al. Steam reforming of ethanol for hydrogen production: influence of catalyst composition (Ni/Al2O3, Ni/Al2O3–CeO2, Ni/Al2O3–ZnO) and process conditions. React Kinet Mech Catal 2021;132:907–19. https://doi.org/10.1007/s11144-021-01945-6.
[119] Ashraf MA, Sanz O, Montes M, Specchia S. Insights into the effect of catalyst loading on methane steam reforming and controlling regime for metallic catalytic

monoliths. Int J Hydrogen Energy 2018;43:11778–92. https://doi.org/10.1016/j.ijhydene.2018.04.126.
[120] Shariatinia Z, Khani Y, Bahadoran F. Synthesis of a novel 3 %Ru/CeZr0.5GdO4 nanocatalyst and its application in the dry and steam reforming of methane. Int J Environ Sci Technol 2016;13:423–34. https://doi.org/10.1007/s13762-015-0907-x.
[121] Roy PS, Park N-K, Kim K. Metal foam-supported Pd–Rh catalyst for steam methane reforming and its application to SOFC fuel processing. Int J Hydrogen Energy 2014;39:4299–310. https://doi.org/10.1016/j.ijhydene.2014.01.004.
[122] Chein R, Yang Z. Experimental study on dry reforming of biogas for syngas production over Ni-based catalysts. ACS Omega 2019;4:20911–22. https://doi.org/10.1021/acsomega.9b01784.
[123] Zhang Z, Bi G, Han B, Liu L, Zhong J, Xie J. Upgrading biogas into syngas via bi-reforming of model biogas over ruthenium-based nano-catalysts synthesized via mechanochemical method. Int J Hydrogen Energy 2023;48:16958–70. https://doi.org/10.1016/j.ijhydene.2023.01.202.
[124] Kokka A, Petala A, Panagiotopoulou P. Support effects on the activity of Ni catalysts for the propane steam reforming reaction. Nanomaterials 2021;11:1948. https://doi.org/10.3390/nano11081948.
[125] Jampa S, Jamieson AM, Chaisuwan T, Luengnaruemitchai A, Wongkasemjit S. Achievement of hydrogen production from autothermal steam reforming of methanol over Cu-loaded mesoporous CeO2 and Cu-loaded mesoporous CeO2–ZrO2 catalysts. Int J Hydrogen Energy 2017;42:15073–84. https://doi.org/10.1016/j.ijhydene.2017.05.022.
[126] Khzouz M, Gkanas EI, Du S, Wood J. Catalytic performance of Ni-Cu/Al2O3 for effective syngas production by methanol steam reforming. Fuel 2018;232:672–83. https://doi.org/10.1016/j.fuel.2018.06.025.
[127] Diaz-Perez MA, Moya J, Serrano-Ruiz JC, Faria J. Interplay of support chemistry and reaction conditions on copper catalyzed methanol steam reforming. Ind Eng Chem Res 2018. https://doi.org/10.1021/acs.iecr.8b02488. acs.iecr.8b02488.
[128] Seung-hoon K, Jae-sun J, Eun-hyeok Y, Kwan-Young L, Dong Ju M. Hydrogen production by steam reforming of biomass-derived glycerol over Ni-based catalysts. Catal Today 2014;228:145–51. https://doi.org/10.1016/j.cattod.2013.11.043.
[129] Ramesh S, Yang E-H, Jung J-S, Moon DJ. Copper decorated perovskite an efficient catalyst for low temperature hydrogen production by steam reforming of glycerol. Int J Hydrogen Energy 2015;40:11428–35. https://doi.org/10.1016/j.ijhydene.2015.02.013.